characteristics, protein synthesis, and induction of cytokine release. Blood **88**: 174–183.

40) van Setten, P.A., van Hinsbergh, V.W., Van den Heuvel, L.P., van der Velden, T.J., van de Kar, N.C., Krebbers, R.J., Karmali, M.A., and Monnens, L.A. 1997. Verocytotoxin inhibits mitogenesis and protein synthesis in purified human glomerular mesangial cells without affecting cell viability: evidence for two distinct mechanisms. J. Am. Soc. Nephrol. **8**: 1877–1888.

41) Yiu, S.C., and Lingwood, C.A. 1992. Polyisobutylmethacrylate modifies glycolipid binding specificity of verotoxin 1 in thin-layer chromatogram overlay procedures. Anal. Biochem. **202**: 188–192.

HYBRIDOMA AND HYBRIDOMICS
Volume 23, Number 3, 2004

Development of Novel Monoclonal Antibody 4G8 against Swine Leukocyte Antigen Class I α Chain

WEI-RAN TANG,[1] NOBUTAKA KIYOKAWA,[1] TOMOKO EGUCHI,[3] JUN MATSUI,[1] HISAMI TAKENOUCHI,[1] DAISUK HONMA,[3] HIROSHI YASUE,[3] SHIN ENOSAWA,[2] KENICHI MIMORI,[1] MITSUKO ITAGAKI,[1] TOMOKO TAGUCHI,[1] YOHKO U. KATAGIRI,[1] HAJIME OKITA,[1] HIROSHI AMEMIYA,[2] and JUNICHIRO FUJIMOTO[1]

ABSTRACT

A mouse monoclonal antibody (MAb) was generated against swine leukocyte antigen (SLA) class I α chain. A newly developed series of MAb clones that react with pan leukocytes were selected and tested by immunohistochemistry using SLA class I α chain expressing Cos-7 cells. Among them, MAb 4G8 was characterized by the following features: (1) 4G8 reacted with Cos-7 cells transfected with SLA class I α chain from the *d* haplotype, (2) 4G8 recognized epitopes that were different from those of commercially available anti-SLA class I MAbs 74-11-10 and PT85A, and (3) 4G8 could be used to immunostain frozen sections of thymus, spleen, lymph node, kidney, and liver tissues with good results.

INTRODUCTION

THE PORCINE SYSTEM has received much attention as a suitable model for transplantation medicine. Therefore, an accurate understanding of human immune responses to porcine tissues has become increasingly important. However, the details of the porcine immune system, especially those features that are novel to the pig, remain unclear. We thus attempted to develop new MAbs that could be used to analyze the porcine immune system.

The immune response to foreign antigens is determined by the expression of specific major histocompatibility complex (MHC) molecules that can bind and present peptide fragments of that protein to T cells. There are two different types of MHC gene products, termed Class I and Class II MHC molecules, and any given T cell recognizes foreign antigens bound to only one Class I or Class II MHC molecule. Antigens associated with Class I molecules are recognized by $CD8^+$ cytolytic T cells, whereas class II–associated antigens are recognized by $CD4^+$ helper T cells. Class I molecules are located on every nucleated cell surface, except those of neurons and trophoblasts. In contrast, the expression of Class II molecules is limited to certain cell types. In pigs, MHC molecules are known as swine leukocyte antigens (SLA). All SLA class I molecules contain two separate polypeptide chains: an MHC-encoded α chain of 45 kD and a non–MHC-encoded β chain of 12 kD.

Recently, the profound involvement of SLA Class I molecules in human anti-porcine cell reactions has been described. Several studies have shown that human T cells can directly recognize porcine MHC molecules and that such recognition can lead to the killing of the porcine cells. Porcine cells have recently been shown, moreover, to be targets for human NK cells. Since human MHC class I molecules deliver a negative signal to human NK cells, protecting syngeneic cells from lysis, we surmised that differences in the gene sequences of porcine MHC class I molecules may be responsible for the lack of recognition by human NK cell receptors and subsequent cytolysis of the porcine cells. In addition, it was reported that a single treatment with a monoclonal antibody (MAb) directed against the SLA class I provides an attractive approach to the induction of T cell tolerance, possibly enabling long-term graft survival in porcine-to-human cell transplantations.[1] These studies indicate that SLA class I molecules play critical roles in transplantation medicine.

Departments of [1]Developmental Biology and [2]Innovative Surgery, National Research Institute for Child Health and Development, Tokyo, Japan.
[3]Genome Research Department, National Institute for Agrobiological Science, Ibayaki, Japan.

Here, we report a novel MAb 4G8 against the SLA class I α chain that was proven to be different from four commercially available anti-SLA class I MAbs. The utilization of 4G8 in tissue sections was also examined.

MATERIALS AND METHODS

Animals and tissues

Landrace or (Landrace × Large White) F1 pigs were used in this study. Peripheral blood (PB) and tissues were obtained from anesthetized animals and were processed. PB was collected in acid citric buffer to avoid coagulation. Tissues were immediately snap frozen and kept in the deep freezer until use.

Monoclonal antibodies

PB leukocytes were treated using RBC lysis with NH_4Cl lysis buffer followed by centrifugation at 1,500 rpm for 10 min. After washing twice in phosphate-buffered saline (PBS), approximately 1×10^8 cells were injected into the abdominal cavity of 8-week-old female Balb/c mice. Boost injections were performed twice at 2-week intervals. At 4 days after the last boost, splenocytes were fused with P3U1 mouse myeloma cells and incubated in hypoxanthine and thymidine (HAT) medium. Supernatants of growing hybridomas were screened on porcine PB leukocytes by flow cytometry and clones secreting antibodies reactive with porcine PB leukocytes were subcloned twice by limiting dilution. Clones were grown in the abdominal cavity of Pristane-treated Balb/c mice, and ascites were obtained. Purification of MAbs was performed by Protein-A or Protein-G column (Bio-Rad Laboratories, Hercules, CA). After purification, MAb was fluorescence isothiocyanate (FITC) conjugated as described previously.[2] Commercially available MAbs against SLA class I 74-11-10, PT85A, H17A*, H58A* (* indicates known as cross-reactive with pig and other species) were obtained from Veterinary Medical Research and Development (Pullman, WA).

Flowcytometry and immunohistochemistry

Flowcytometrical analysis of MAbs was carried out as follows. Briefly, aliquot of porcine PB was incubated with appropriate amount of MAb for 30 min at 4°C. After washing with PBS, cells were incubated with FITC-conjugated (Jackson Laboratory, West Grove, PA) for 30 min at 4°C. Cells were washed with PBS and analyzed by EPICS XL analyzer (Beckman/Coulter, Westbrook, MA).

Reactivity of MAbs on tissues were analyzed by immunohistochemistry on frozen sections. Briefly, porcine tissues were snap-frozen in optimal cutting temperature (OCT) compounds and frozen sections were made by cryostat apparatus. Sections were fixed by acetone for 15 min at 4°C. After washing in PBS and blocked with normal rabbit serum, sections were incubated with MAbs at appropriate dilutions for 30 min at room temperature. Sections were then washed with PBS and incubated with horseradish peroxidase (HRP)–conjugated rabbit anti-mouse antibodies (Jackson Laboratory) for 30 min at room temperature. After washing with PBS, color development was done in diaminobenzidine solution (10 mM in 0.05 M Tris-HCl, PH 7.5) with 0.003% H_2O_2.

Binding competition assay

Binding competition assay was carried out as follows. Briefly, after aliquot of porcine PB leukocytes were incubated with 2ug saturated amount of commercially available MAbs for 30 min at 4°C. The cells saturated with these commercially available MAbs were stained with FITC-4G8 for 30 min at 4°C. Then, PB leukocytes were treated using RBC lysis with NH_4Cl lysis buffer followed by centrifugation at 1,500 rpm for 10 min. FITC-mouse immunoglobulin (MsIg) was used as control antibody. Cells were washed with PBS and analyzed by EPICS XL analyzer (Beckman/Coulter).

Cloning and expression of porcine cDNA library

As another purpose for analysis of γδTCR against MAb (7G3) and CD8 against MAb (6F10), cDNA libraries of 7G3-positive as well as 6F10-positive PB leukocytes were first constructed. A brief description is shown below. Porcine PB labeled with FITC-7G3 antibody was incubated with magnetic-activated cell sorting (MACS) beads conjugated with anti-FITC antibody (Miltenyi Biotec, Bergisch Gladbach, Germany) and was loaded onto AutoMACS cell separator (Miltenyi Biotec). 7G3-positive cells were positively selected and a cDNA library was constructed using the oligo-capping method[3] and plasmid vector pME18S-FL3, which contains the SR-α promoter for expression in mammalian cells. To 7G3-negative pass-through fractions, FITC-6F10 was added and labeled. These cells were also positively selected by AutoMACS and used for the cDNA library construction. Out of several thousand clones sequenced from both cDNA libraries, one clone was selected which exhibited homologies to known porcine MHC class I sequences from d haplotype and contained full-length open reading frames.

Complementary DNA coding for porcine MHC class I under SRα promoter was introduced into COS7 cells by lipofec-

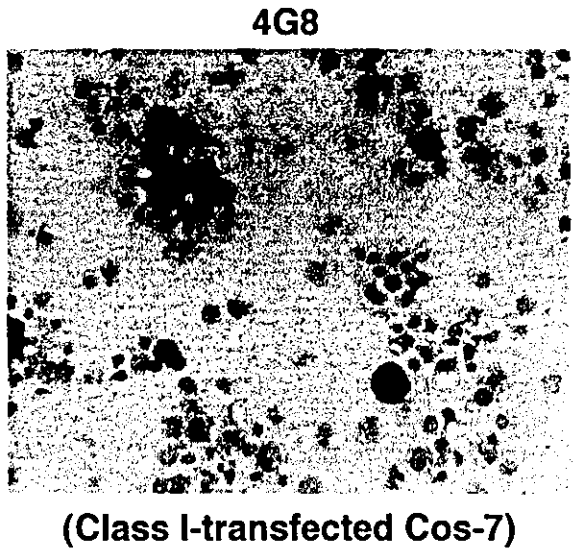

FIG. 1. Reactivity of 4G8 on Cos-7 cells transfected with SLA class I PD1. Mammalian expression vectors containing SLA class I PD1 were introduced into Cos-7 cells, and the cells were stained with 4G8 using immunohistochemistry.

tion (LIPOFECTAMIN, Invitrogen, Groningen, Netherlands) and cells were stained with 4G8 MAb after 3 days.

RESULTS AND DISCUSSION

Anti-SLA Class I MAb 4G8 recognizes a distinct epitope from those of commercially available antibodies

From one hybridization experiment, 45 hybridoma clones were established. The MAbs produced by these clones reacted differently to the porcine PB leukocytes, as revealed by flow cytometry (data not shown). To determine whether a MAb against SLA class I α chain was included among these clones, MAb clones that reacted with pan leukocytes were selected and tested by immunohistochemistry using SLA class I α chain expressing Cos-7 cells. As shown in Figure 1, when a mammalian expression vector of SLA class I PD1 from d haplotype was transfected into Cos-7 cells, clone 4G8 was found to stain the cells, whereas control MsIg failed to stain the cells (data not shown). Therefore, 4G8 was considered to recognize the SLA class I α chain, including the d haplotype.

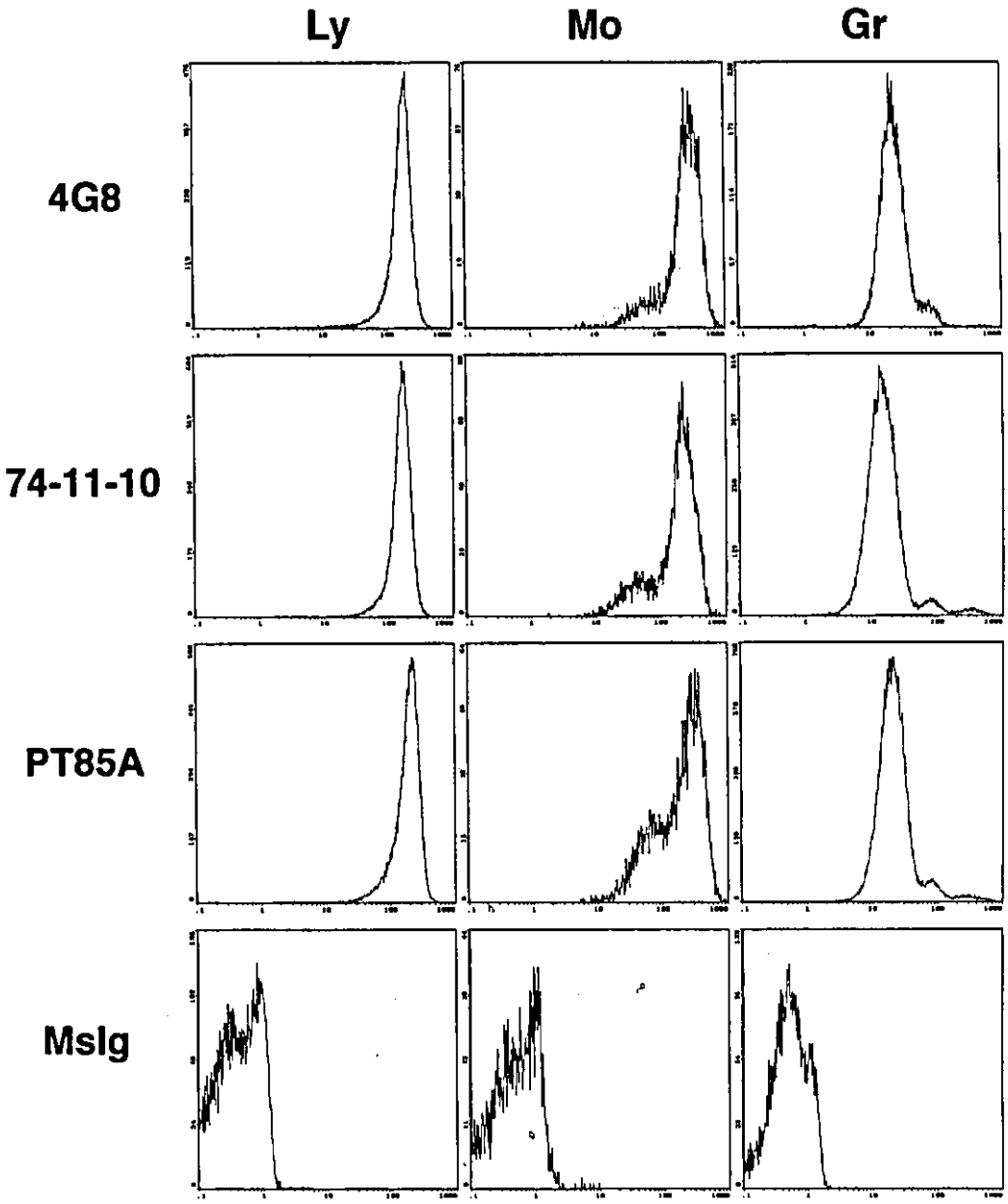

FIG. 2. Comparison of reactivity profiles of 4G8 and commercially available anti-SLA class I monoclonal antibodies. Porcine PB leukocytes were stained with 4G8 and commercially available anti-SLA class I MAbs, 74-11-10, and PT85A, using flow cytometry. MsIg was used as a control antibody.

Next, we compared the reactivity of 4G8 with commercially available anti-SLA class I Abs 74-11-10, PT85A, H17A, H58A to PB from outbred domestic pigs. As shown in Figure 2, flow-cytometrical analysis demonstrated that the reactivity of 74-11-10 and PT85A to the porcine PB was similar to that of 4G8. Although multiple samples from individual animals were tested, all of these MAbs always revealed a pan leukocyte positive staining pattern. In contrast, H17A did not react with the domestic porcine PB samples (data not shown), indicating that H17A is polymorphic in pigs. H58A, exhibited variable reactivity from one animal to another (data not shown). This data indicates that the reactivity of H17A and H58A is different from that of 4G8.

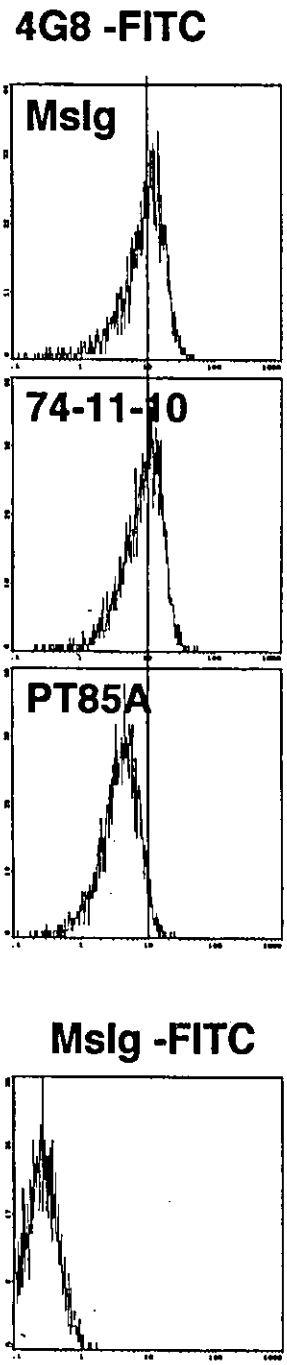

FIG. 3. Competition binding assay using flow cytometry. 4G8 continued to react with porcine PB leukocytes that had been saturated with commercially available MAbs (74-11-10 and PT85A). MsIg-FITC was used as a negative control.

To determine whether the epitope recognized by 4G8 was the same as that of 74-11-10 and PT85A, we examined whether 4G8 could still bind to the cells after the cells had been saturated with 74-11-10 or PT85A. As shown in Figure 3, 4G8 continued to react with PB leukocytes that had been saturated with 74-11-10 or PT85A. These results indicate that 4G8 recognizes a novel epitope distinct from those recognized by 74-11-10, PT85A, H17A and H58A. MHC class I molecules are extremely polymorphic, and polymorphism often occurs in the $\alpha 1$ domain, or the $\alpha 2$ domain, but the $\alpha 3$ domain is nonpolymorphic.[4] 74-11-10 and PT85A have been reported to require the PD1 $\alpha 1/\alpha 2$ domains, but not the $\alpha 3$ domain, to exhibit reactivity.[1] A precise analysis to clarify which domain is recognized by 4G8 is now underway.

Analysis of 4G8 using immunohistochemistry

We examined whether 4G8 could be used to immunostain frozen sections. As shown in Figure 4, 4G8 produced high-quality immunostaining results when used on frozen sections. In thymus tissues, 4G8 produced a dense and diffuse staining pattern in the medullar region and a lighter, scattered staining pattern in the cortex, suggesting that SLA class I molecules are mainly expressed on mature thymocytes in the medulla, but not on immature thymocytes in the cortex. In spleen, lymph node, kidney and liver tissues, 4G8 produced an ubiquitous staining pattern, as shown in Figure 4. These results demonstrate that 4G8 can be effectively used to immunostain frozen sections. Therefore, 4G8 may be a useful reagent for immunopathology studies and improving our general understanding of the porcine immune system.

In conclusion, a novel MAb, 4G8, that recognizes the SLA class I α chain has been identified and used to produce high-quality immunostaining results on tissues sections. 4G8 is expected to become a useful tool for investigating the immune system of domestic pigs.

ACKNOWLEDGMENTS

We thank M. Sone and S. Yamauchi for their excellent secretarial work. This research was supported in part by Health and Labor Sciences Research Grants from the Ministry of Health, Labor and Welfare of Japan and MEXT (KAKENHI 15019129, JSPS. KAKENHI 15390133 and 15590361). Support was also provided by a grant from the Japan Health Sciences Foundation for Research on Health Sciences Focusing on Drug Innovation and a grant from the Sankyo Foundation of Life Science.

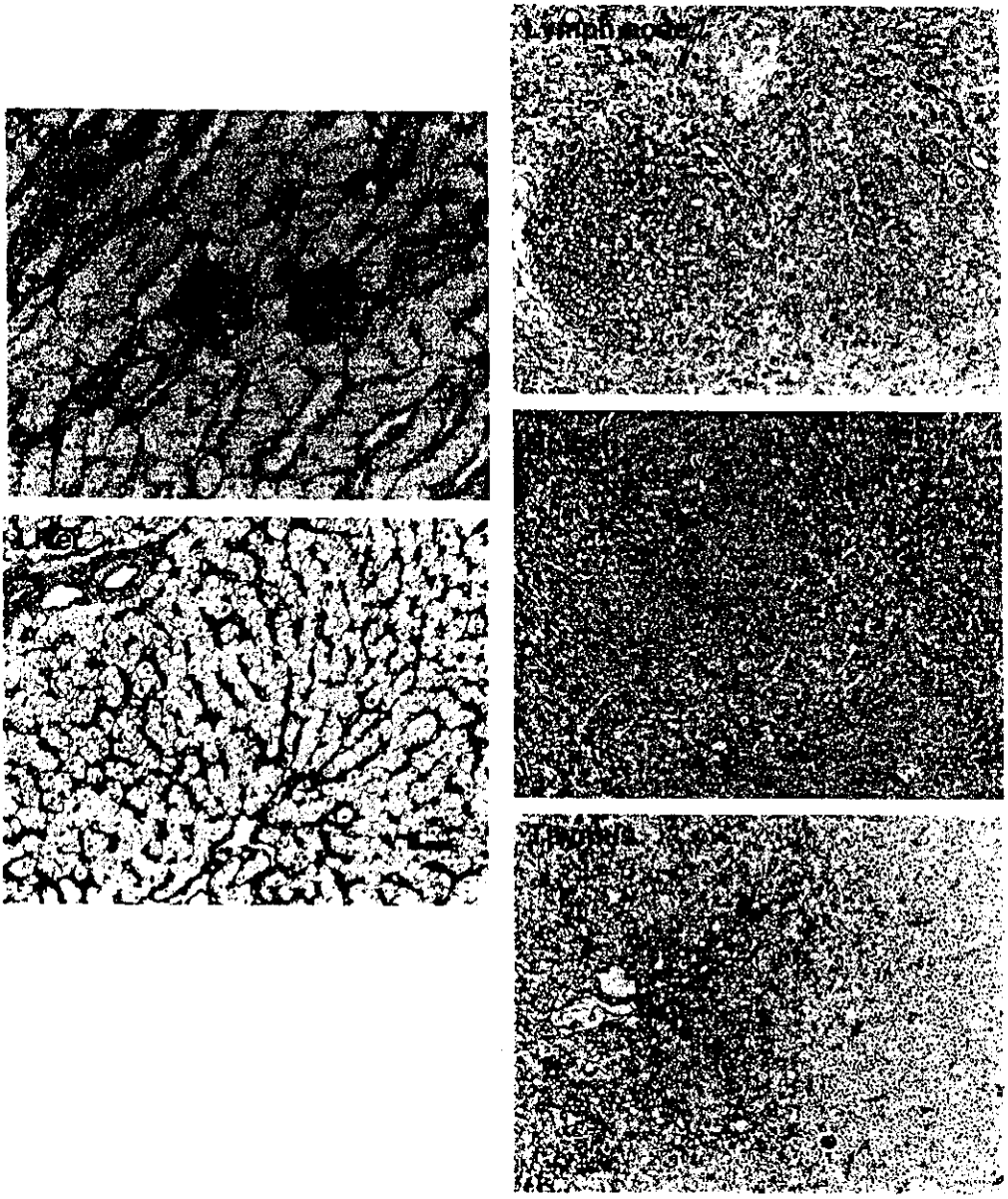

FIG. 4. Reactivity of 4G8 on frozen sections of porcine tissues. Frozen sections of porcine thymus, spleen, lymph node, kidney, and liver tissues were stained with 4G8 using immunohistochemistry.

REFERENCES

1. DerSimonian H, Pan L, Yatko C, Rodrigue-Way A, Johnson E, and Edge AS: Human anti–porcine T cell response: blocking with anti–class I antibody leads to hyporesponsiveness and a switch in cytokine production. J Immunol 1999;162:6993–7001.
2. Fujimoto J, Ishimoto K, Kiyokawa N, Tanaka S, Ishii E, and Hata J: Immunocytological and immunochemical analysis on the common acute lymphoblastic leukemia antigen (CALLA): evidence that CALLA on ALL cells and granulocytes are structurally related. Hybridoma 1988;7:227–236.
3. Maruyama K, and Sugano S: Oligo-capping: a simple method to replace the cap structure of eukaryotic mRNAs with oligoribonucleotides. Gene 1994;138:171–174.
4. Sullivan JA, Oettinger HF, Sachs DH, and Edge AS: Analysis of polymorphism in porcine MHC class I genes: alterations in signals recognized by human cytotoxic lymphocytes. J Immunol 1997;159: 2318–2326.

Address reprint requests to:
Junichiro Fujimoto, Ph.D.
Department of Developmental Biology
National Research Institute for Child Health and Development
3-35-31, Taishido, Setagaya-ku
Tokyo 154-8567, Japan

E-mail: jfujimoto@nch.go.jp

Received for publication February 27, 2004. Accepted for publication March 24, 2004.

Shiga toxin binding to globotriaosyl ceramide induces intracellular signals that mediate cytoskeleton remodeling in human renal carcinoma-derived cells

Hisami Takenouchi[1,2], Nobutaka Kiyokawa[1,*], Tomoko Taguchi[1], Jun Matsui[1], Yohko U. Katagiri[1], Hajime Okita[1], Kenji Okuda[2] and Junichiro Fujimoto[1]

[1]Department of Developmental Biology, National Research Institute for Child Health and Development, 3-35-31, Taishido, Setagaya-ku, Tokyo, 154-8567, Japan
[2]Department of Bacteriology, Yokohama City University School of Medicine, 3-9 Fukuura, Kanazawa-ku, Yokohama 236-0004, Japan
*Author for correspondence (e-mail: nkiyokawa@nch.go.jp)

Accepted 6 April 2004
Journal of Cell Science 117, 3911-3922 Published by The Company of Biologists 2004
doi:10.1242/jcs.01246

Summary

Shiga toxin is a bacterial toxin consisting of A and B subunits. Generally, the essential cytotoxicity of the toxin is thought to be mediated by the A subunit, which possesses RNA cleavage activity and thus induces protein synthesis inhibition. We previously reported, however, that the binding of the Shiga toxin 1-B subunit to globotriaosyl ceramide, a functional receptor for Shiga toxin, induces intracellular signals in a manner that is dependent on glycolipid-enriched membrane domains, or lipid rafts. Although the precise role of this signaling mechanism is not known, here we report that Shiga-toxin-mediated intracellular signals induce cytoskeleton remodeling in ACHN cells derived from renal tubular epithelial carcinoma. Using confocal laser scanning microscopy, we observed that Shiga toxin 1-B treatment induces morphological changes in ACHN cells in a time-dependent manner. In addition, the morphological changes were accompanied by the redistribution of a number of proteins, including actin, ezrin, CD44, vimentin, cytokeratin, paxillin, FAK, and α- and γ-tubulins, all of which are involved in cytoskeletal organization. The transient phosphorylation of ezrin and paxillin was also observed during the course of protein redistribution. Experiments using inhibitors for a variety of kinases suggested the involvement of lipid rafts, Src family protein kinase, PI 3-kinase, and RHO-associated kinase in Shiga toxin 1-B-induced ezrin phosphorylation. Shiga toxin 1-B-induced cytoskeletal remodeling should provide an in vitro model that can be used to increase our understanding of the pathogenesis of Shiga-toxin-mediated cell injury and the role of lipid-raft-mediated cell signaling in cytoskeletal remodeling.

Key words: Shiga toxin, Globotriaosylceramide, Cytoskeleton

Introduction

Shiga toxin (Stx) is a protein toxin produced by Stx-producing strains of *Escherichia coli* (STEC) and has been postulated to be the substance responsible for the development of serious complications associated with STEC infection, such as hemolytic uremic syndrome (HUS) (Kaplan et al., 1990; Richardson et al., 1988). Stx consists of two major types, Stx1 and Stx2, that both contain an A-subunit monomer and a B-subunit pentamer (Lingwood, 1996). The A-subunit is a 30 kDa cytotoxic chain that exhibits RNA *N*-glycohydrolase activity and cleaves a specific adenine residue on the 28S ribosomal RNA in the cytosol, thereby inhibiting protein synthesis (Lingwood, 1996). In contrast, the 7 kDa B-subunit can bind to globotriaosyl ceramide (Gb3), the functional receptor for Stx found on the surface of target cells (Lingwood, 1996). Although Stx cytotoxicity is thought to be caused by the A-subunit-mediated inhibition of protein synthesis, a number of recent studies have clarified that the B-subunit also has a biological effect on the target cells.

For example, Stx-B binding to Gb3 has been shown to trigger intracellular signaling events in Burkitt's lymphoma cells (Taga et al., 1997). We further observed that Gb3 was only distributed in glycolipid-enriched membrane (GEM) domains (Rodgers and Rose, 1996), also known as lipid rafts (Simons and Ikonen, 1997), indicating that lipid rafts are deeply involved in Stx-mediated signal transduction in both Burkitt's lymphoma cells (Mori et al., 2000) and renal carcinoma ACHN cells (Katagiri et al., 1999). However, the physiological role of Gb3-mediated cell signaling remains unknown. Although Stx1-B binding is sufficient to induce apoptosis in Burkitt's lymphoma cells (Kiyokawa et al., 2001; Mangeney et al., 1993; Taga et al., 1997), this effect of Stx1-B appears to be limited to this species of cells, and the A-subunit of Stx is reportedly required to induce apoptosis in other cell types, including Vero cells and monocytic THP-1 cells (Kojio et al., 2000; Williams et al., 1997).

Ezrin, radixin and moesin are members of the ERM protein family and are mainly distributed just beneath the plasma membranes of cellular protrusions, such as microvilli. ERM proteins are thought to function as general cross-linkers between plasma membranes and actin filaments (Arpin et al., 1994; Bretscher et al., 1997; Tsukita and Yonemura, 1997; Tsukita et al., 1997; Tsukita and Yonemura, 1999). The highly conserved NH2-terminal halves of ERM proteins possess the

ability to associate with several integral membrane proteins, such as CD43, CD44, intercellular adhesion molecule (ICAM)-1, ICAM-2, ICAM-3, and the H^+/K^+ ATPase pump (Bretscher et al., 1997; Heiska et al., 1998; Hirao et al., 1996; Serrador et al., 1997; Tsukita et al., 1994; Tsukita and Yonemura, 1999; Yonemura et al., 1993). Conversely, the COOH-terminal halves of ERM proteins can interact with actin filaments (Bretscher et al., 1997; Tsukita and Yonemura, 1999; Turunen et al., 1994). As the NH2-terminal halves of ERM proteins can also bind to their COOH-terminal halves (Andreoli et al., 1994; Bretscher et al., 1997; Tsukita and Yonemura, 1999), both the actin- and membrane-binding domains of ERM proteins are thought to be masked in the resting state by an intramolecular and/or intermolecular head-to-tail association (Berryman et al., 1995; Bretscher et al., 1995; Bretscher et al., 1997; Tsukita and Yonemura, 1999). These dormant ERM proteins are thought to be activated by cellular signals, such as the one mediated by epidermal growth factor receptor, by exposing their halves and allowing them to interact with integral membrane proteins and actin filaments, respectively (Berryman et al., 1995; Bretscher et al., 1995; Bretscher et al., 1997; Hirao et al., 1996; Matsui al., 1998; Tsukita and Yonemura, 1999). These activated ERM proteins have been shown to be directly involved in the morphogenesis of the free surface domain of plasma membranes, especially in the organization of microvilli (Berryman et al., 1995; Bretscher et al., 1997; Chen et al., 1995; Crepadi et al., 1997; Kondo et al., 1997; Takeuchi et al., 1994; Tsukita and Yonemura, 1999).

In this study, we investigated the effect of Stx1-B binding to Gb3 on ACHN cells and found that an intracellular signal mediated by Gb3 induces the phosphorylation of ezrin proteins, leading to a reorganization of the cytoskeleton and morphological changes. Our findings should improve our understanding of the molecular mechanism of Stx-mediated cell damage and the functional roles of Gb3-mediated intracellular signals in a physiological context.

Materials and Methods

Materials

The Stx1-B pentamer was prepared as described previously (Nakajima et al., 2001). The mouse monoclonal antibodies (mAbs) d in this study were obtained from BD Biosciences (Lexington, KY) (anti-ezrin, anti-paxillin and anti-Yes), Immunotech (Fullerton, CA) (anti-CD44 and anti-cytokeratin), Affinity BioReagents, Inc. (ABR, Golden, CO) (anti-vimentin), Santa Cruz Biotechnology (Santa Cruz, CA) (anti-actin), and Sigma-Aldrich Fine Chemicals (St Louis, MO) (anti-α Tubulin). The mouse anti-Gb3 mAb 1A4 was a generous gift of S. Hakomori of the University of Washington (Seattle, WA) and Otsuka Assay Laboratories (Kawauchi-cho, Tokushima, Japan). The rat anti-Gb3 mAb 38.13 were obtained from Immunotech. The polyclonal Abs were obtained from Upstate biotechnology (Lake Placid, NY) (anti-FAK), New England Biolabs, (Bevely, MA) (anti-phospho-specific ezrin and anti-phospho-specific paxillin), ABR (anti-phospho-specific Src) and Sigma (anti-γ Tubulin). Peroxidase-conjugated secondary Abs were purchased from DAKO (Glostrup, Denmark). Fluorescence-conjugated secondary Abs and fluorescence labeling reagents for the primary Abs were purchased from Molecular Probes, Inc. (Eugene, OR). The Rho-dependent serine/threonine kinase (ROCK) inhibitor Y-27632, PI 3 kinase (PI3K) inhibitor LY-294002, protein kinase C (PKC) inhibitor 20-28, PKC inhibitor EGF-R fragment 651-658, and Src family protein tyrosine kinase (PTK) inhibitor PP2 were purchased from Calbiochem-Novabiochem (San Diego, CA). Methyl-β-cyclodextrin (MBD) and DAPI were obtained from Sigma. TRITC-conjugated phalloidin was purchased from Molecular Probes. Cell-tracker Green was also purchased from Molecular Probes. Other chemical reagents were obtained from Wako Pure Chemical Industries (Osaka, Japan), unless otherwise indicated.

Cell culture

Renal tubular epithelial carcinoma-derived ACHN cells that were sensitive to Stx1 cytotoxicity (Katagiri et al., 1999; Taguchi et al., 1998) were used in this study. The cells were maintained in DMEM supplemented with 10% FCS at 37°C in a humidified 5% CO_2 atmosphere. Cells were grown to approximately 75% confluence and stimulated. In most of the experiments, Stx1-B pentamer was directly added to the culture medium at a concentration of 5.0 μg/ml and cells were incubated for the time periods indicated in the figures, unless otherwise indicated.

Immunohistochemistry and confocal microscopic analysis

To observe cell morphology, ACHN cells were plated on a polylysine-coated glass bottom dish (Matsunami Glass, Tokyo, Japan) and labeled with Cell-tracker Green, according to the manufacturer's protocol. For the immunohistochemical staining, the cells were plated on a collagen-coated cover slip (Iwaki Glass, Tokyo, Japan). After each treatment, cells on cover slips were washed with ice–cold PBS and fixed with ice-cold acetone for 20 minutes at 4°C, then stained with each combination of Abs and/or reagents described below.

For the simultaneous detection of ezrin and filamentous actin (F-actin), the cover slips were incubated with primary Abs against ezrin (5 μg/ml) at room temperature for 30 minutes followed by PBS washing. The cells were further incubated with secondary goat anti-mouse Ab labeled with Alexa Fluor® 488 (1:300 dilution) for 30 minutes, followed by PBS washing and then stained with DAPI (200 ng/ml) and TRITC-conjugated phalloidin (5 units/ml) (Knowles and McCulloch, 1992). The detection of CD44 and F-actin was performed similarly.

For the detection of paxillin and FAK, a combination of mouse anti-paxillin mAb and rabbit anti-FAK polyclonal Ab was used. Both primary Abs (5 μg/ml each) were detected by Alexa Fluor® 488-conjugated goat anti-mouse Ab and Alexa Fluor® 546-conjugated goat anti-rabbit Ab (1:300 each), respectively. Each secondary Ab was highly cross-absorbed, thus the cross reactions were not detected in preliminary experiments (data not shown). The detection of α- and γ-tubulin was performed similarly. For the simultaneous detection of vimentin and cytokeratin, each primary Ab was labeled using either the Alexa Fluor® 488 Protein Labeling Kit or the Zenon™ Alexa Fluor® 546 Mouse IgG1 Labeling Kit.

Confocal laser scanning was performed using a FV500 confocal laser scanning microscope (Olympus, Tokyo, Japan). Simultaneous multi-fluorescence acquisitions were performed using the 351 nm, 488 nm, and 543 nm laser lines to excite DAPI, Alexa Fluor™488 and Alexa Fluor™546 (TRITC), respectively, using a water immersion objective (×40, NA1.7). Fluorescent images were selected using appropriate multi-fluorescence dichroic mirrors and band pass filters using the sequential acquisition mode.

Immunoblot analysis

For the immunoblot analysis, ACHN cells were plated on a 100 mm culture dish (Corning, Corning, NY). Cell lysates were prepared by solubilizing cells in 400 μl of lysis buffer, and the protein concentration of each cell lysate was determined as described previously (Kiyokawa et al., 2001). 50 μg of each whole cell lysate was electrophoretically separated on an SDS-polyacrylamide gel and transferred to a nitrocellulose membrane using a semi-dry transblot

system (Bio-Rad Laboratories, Hercules, CA). Immunoblotting was performed as described previously (Kiyokawa et al., 2001).

Actin and tubulin polymerization assay

Quantification of actin polymerization was carried out essentially as described previously with minor modifications (Heacock and Bamburg, 1983; Glogauer et al., 1997; McCormack et al., 1999). Briefly, ACHN cells were plated in quintuple wells of a 6-well culture dish (Corning) at 1.5×10^5 cells in 5 ml of medium, and grown for 40 hours to achieve approximately 75% confluence, and treated with 5.0 μg/ml of Stx1-B pentamer for the time periods indicated in the figures. At the end of the incubation period, cells were washed in ice-cold PBS and quickly lysed in 500 μl of actin stabilization buffer (Heacock and Bamburg, 1983; McCormack et al., 1999), a buffer that stabilizes both monomer actin (G-actin, soluble) and F-actin (polymerized) pools. Aliquots of 50 μl from each original (whole) lysate were removed and stored for the determination of total actin. The cell lysates were immediately centrifuged at room temperature for 1 minute in a microcentrifuge at 10,000 *g*, after which the supernatants (G-actin) were removed from the pellets (F-actin). Then 450 μl of actomyosin extraction buffer (Heacock and Bamburg, 1983) was added to the solid pellets. Aliquots of 5 μl from both original lysates (total actin) and resuspended pellets (F-actin) were examined by immunoblot analysis using anti-actin mAb and quantified by densitometry (Glogauer et al., 1997). The proportion of F-actin to total actin was calculated and shown as a percentage.

Quantification of tubulin polymerization was examined essentially the same as actin polymerization with some exceptions. First, the original lysates were prepared by using specific lysis buffer for tubulin and centrifuged at 10,000 *g* for 10 minutes as described elsewhere (Minotti et al., 1991; Montgomery et al., 2000). Second, after removal of the supernatants containing soluble tubulin, solid pellets containing polymerized tubulin were resuspended in water (Minotti et al., 1991; Montgomery et al., 2000). Third, immunoblot analysis was performed with anti-α tubulin mAb.

Results

Morphological changes in ACHN cells induced by Stx1-B treatment

We previously observed, during a study on the biological function of the Stx1-B subunit, that Stx1-B treatment induces a weakening in the adhesion of ACHN cells to the culture dish (Katagiri et al., 2001). As the same phenomenon is also observed in primary cultures of normal human renal cortical epithelial cells (data not shown), it is likely that this is a common feature observed in renal epithelial-derived cells mediated by Stx1-B-induced intracellular signals.

To examine the effect of Stx1-B on the adhesiveness of ACHN cells in greater detail, we stained the cells with Cell-tracker Green and observed the morphological changes using confocal laser scanning microscopy. As shown in Fig. 1, the addition of Stx1-B to the culture weakened the adhesiveness of the cells, as recognized by the increase in intracellular spaces in a time-dependent manner and by the morphological changes, in which the cells became smaller and rounder. In addition, filopodia- and lamellipodia-like structures were temporarily observed after Stx1-B treatment (Fig. 1, arrowhead).

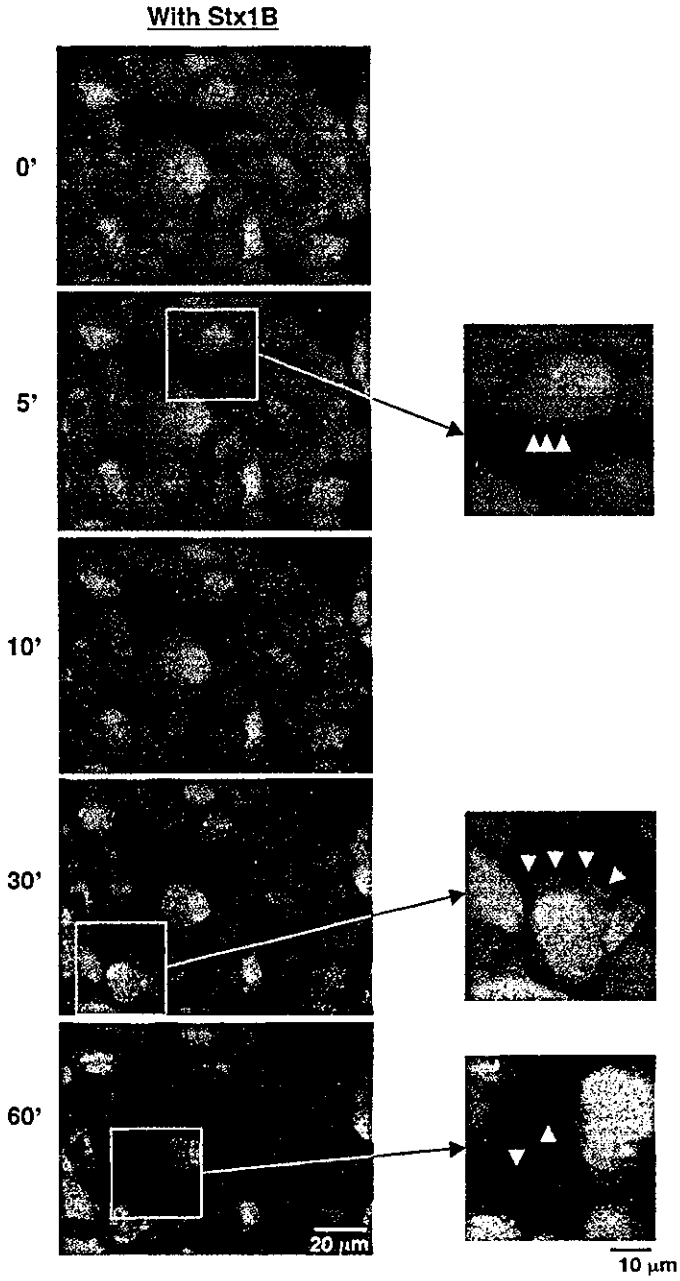

Fig. 1. Morphological changes in ACHN cells after treatment with the Stx1-B subunit. ACHN cells stained with Cell-tracker Green were treated with and without 5 μg/ml of the Stx1-B subunit for the indicated periods and visualized using confocal microscopy. Filopodia- and lamellipodia-like structures are visible at higher magnifications and are indicated by the arrowheads. Results are representative of three independent experiments.

Stx1-B induces the redistribution of cytoskeletal proteins in ACHN cells

The remodeling of cytoskeletal proteins, including the ERM family proteins and actin, is involved in the formation of filopodia or lamellipodia during morphological changes (Berryman et al., 1995; Bretscher et al., 1997; Chen et al., 1995; Crepadi et al., 1997; Kondo et al., 1997; Takeuchi et al., 1994; Tsukita and Yonemura, 1999). Therefore, we examined whether Stx1-B treatment affects the distribution of ezrin and actin. In the resting state, most of the ezrin protein was dispersed in the cytoplasm and only a portion of the protein

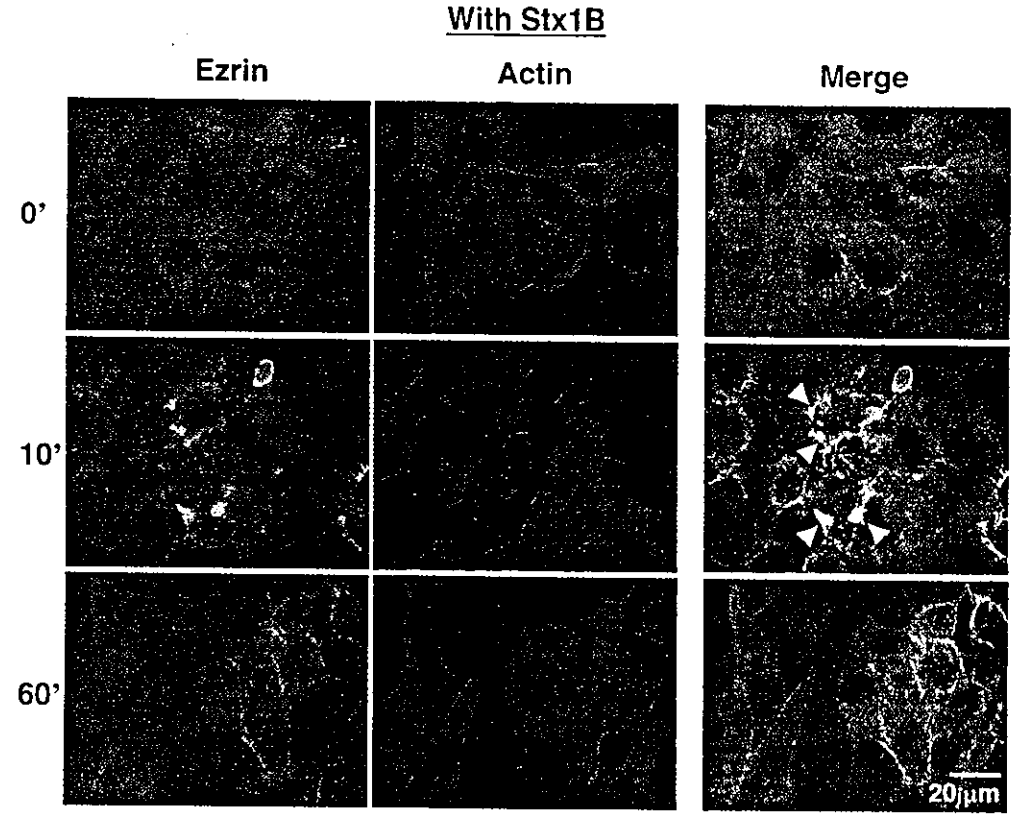

Fig. 2. Effect of Stx1-B subunit on the distribution of ezrin and actin in ACHN cells. ACHN cells treated with the Stx1-B subunit as described in Fig. 1 were double-stained with Alexa-488-labeled anti-ezrin mAb (left panels, green) and TRITC-phalloidin (center panels, red) and visualized using confocal microscopy. The right panels represent the superposition of the green and red images, with DAPI counter staining (blue). The arrowheads indicate the areas of ezrin and actin colocalization (yellow). Results are representative of five independent experiments.

was concentrated in the margin of the cells, as revealed by the brush-like meshwork (Fig. 2, top panels). However, Stx1-B treatment induced a transient enhancement in the concentration of ezrin just beneath the plasma membrane (Fig. 2). Occasionally, the protein clustering peaked at 10 minutes after Stx1-B stimulation (Fig. 2). In parallel, the cortical actin filaments were temporarily polymerized and appeared as thick bundles at the margin of the cells (Fig. 2). The colocalization of both proteins peaked at 10 minutes after Stx1-B stimulation (Fig. 2, yellow area, indicated by arrowhead).

As ERM proteins are thought to play a central role in the organization of cortical actin-based cytoskeletons through the cross-linking of actin filaments and integral membrane, such as CD44 (Tsukita et al., 1994; Tsukita and Yonemura, 1999), we next examined the changes in the distribution of CD44 induced by Stx1-B treatment. As with ezrin, Stx1-B treatment temporarily enhanced the concentration of CD44 in the cell membrane of ACHN cells (Fig. 3). Dual staining with CD44 and F-actin revealed a significant colocalization of both proteins that peaked at 10 minutes after Stx1-B stimulation (Fig. 3, yellow area, indicated by arrowhead).

Paxillin and FAK have been shown to be important for the focal adhesion of cells and growth factor-induced morphological changes (Burridge et al., 1992; Leventhal et al., 1997). Therefore, we examined the effect of Stx1-B stimulation on the distribution of FAK and paxilin. As shown in Fig. 4, most of the FAK and paxillin proteins were independently disseminated throughout the cytoplasm, while small portions of both proteins were colocalized and concentrated within a distinct radial streak at the edges of the cell lamella (yellow area). Upon the addition of Stx1-B, however, the colocalization of FAK and paxillin was temporally enhanced, peaking at 10 minutes after stimulation (Fig. 4, arrowhead).

We further examined the effect of Stx1-B stimulation on other cytoskeletal proteins. The distributions of vimentin and cytokeratin were similar, appearing as a diffuse localization with radial meshwork in the cytoplasm of resting ACHN cells (Fig. 5). Upon Stx1-B stimulation, however, both proteins were temporary concentrated within a paranuclear lesion, peaking at 30 minutes after stimulation in a synchronous manner (Fig. 5, arrowhead).

When the distribution of tubulins was examined using fluorescence immunohistochemistry, a fine mesh work of α-tubulin was seen within the cytoplasm of ACHN cells (Fig. 6). Upon Stx1-B stimulation, the α-tubulin filaments became significantly polymerized, appearing as a thickening of the bundles throughtout the entire cytoplasm and peaking at 10 minutes after stimulation (Fig. 6). Conversely, γ-tubulin was found in cytoplasmic complexes identified as fine spots and specifically concentrated at microtubule-organizing centers (Moritz and Agard, 2001) (Fig. 6). Although the distribution of γ-tubulin did not change significantly after Stx1-B stimulation, a slight enhancement at the microtubule-organizing centers was observed (Fig. 6, arrowhead).

All above observations on Stx1-B-induced cytoskeletal remodeling are entirely based on imaging studies. Therefore, we next examined F-actin formation after Stx1-B stimulation by biochemical means. For this purpose, cell lysate prepared by using actin stabilization buffer was centrifuged and F-actin fraction was separated from soluble G-actin fraction as the pellet. As shown in Fig. 7A, quantification by densitometry of

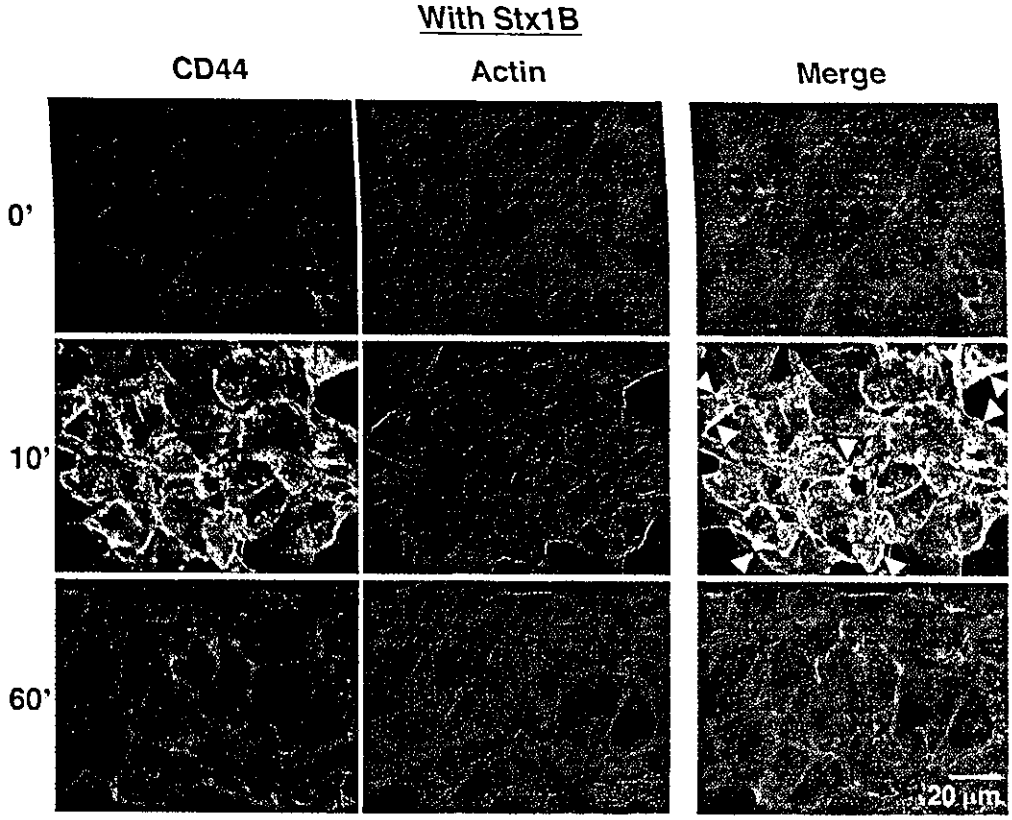

Fig. 3. Effect of Stx1-B subunit on the distribution of CD44 and actin in ACHN cells. ACHN cells were examined as described in Fig. 2 using Alexa-488-labeled anti-CD44 mAb (left panels, green) and TRITC-phalloidin (center panels, red). The arrowheads indicate the areas of CD44 and actin colocalization (yellow). Results are representative of three independent experiments.

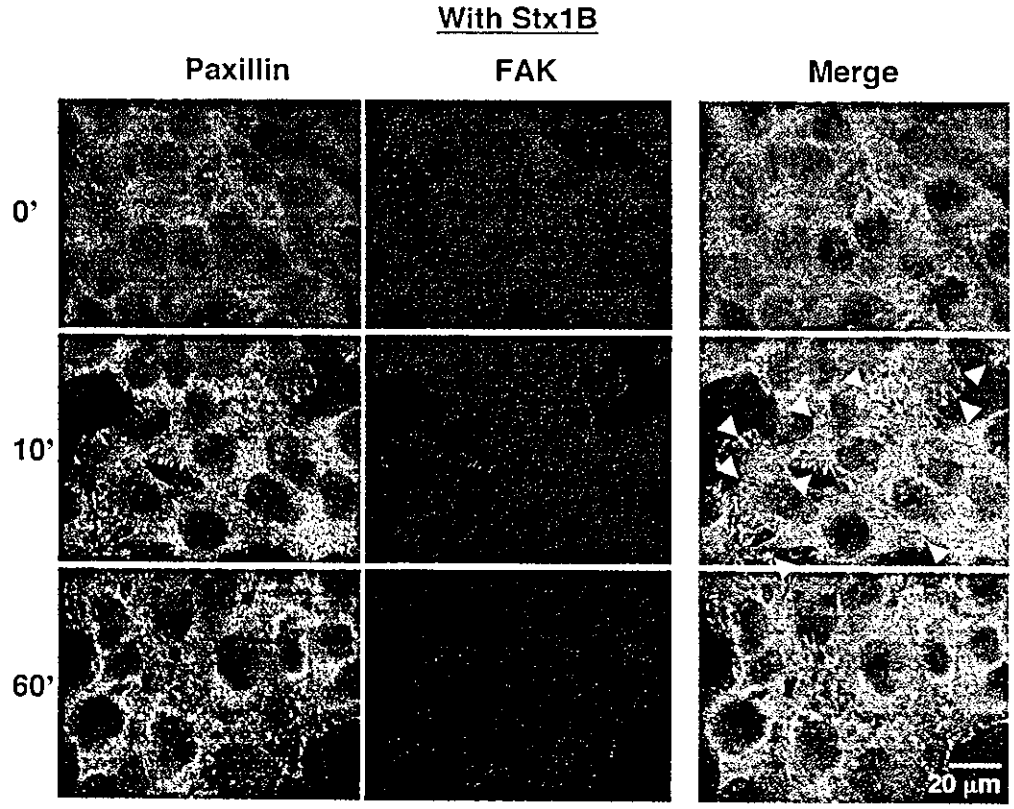

Fig. 4. Effect of Stx1-B subunit on the distribution of paxillin and FAK in ACHN cells. ACHN cells were examined as described in Fig. 2 using Alexa-488-labeled anti-paxillin mAb (left panels, green) and Alexa-546-labeled anti-FAK Ab (center panels, red). The arrowheads indicate the areas of paxillin and FAK colocalization (yellow). Results are representative of three independent experiments.

immunoblots revealed a transient increase in the amount of F-actin fraction, which peaked at 10 to 30 minutes after Stx1-B stimulation. These data coincide with those observed by confocal microscopy experiments using fluorescently labeled phalloidin as a probe for F-actin (Figs 2, 3). We also examined tubulin polymerization similarly. As shown in Fig. 7B, Stx1-

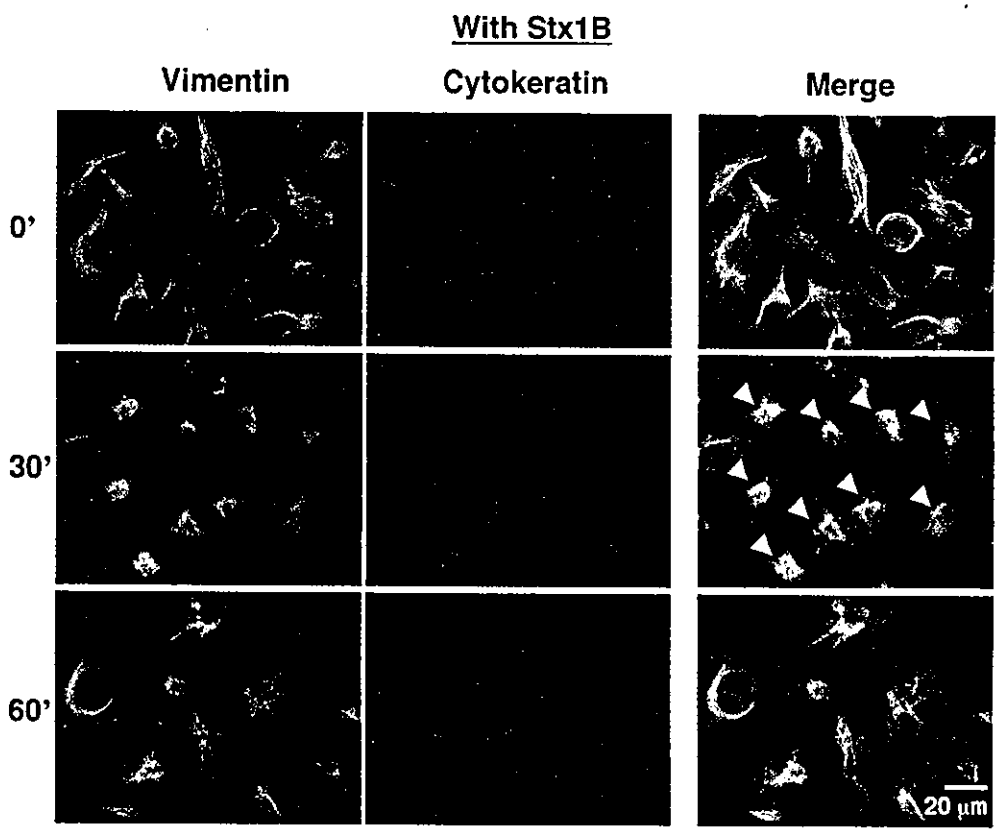

Fig. 5. Effect of Stx1-B subunit on the distribution of vimentin and cytokeratin in ACHN cells. ACHN cells were examined as described in Fig. 2 using Alexa-488-labeled anti-vimentin mAb (left panels, green) and Alexa-546-labeled anti-cytokeratin mAb (center panels, red). The arrowheads indicate the perinuclear clustering of vimentin. Results are representative of three independent experiments.

B-induced transient tubulin polymerization was also confirmed by quantitative analysis.

Stx1-B induces transient phosphorylation of ezrin

The phosphorylation of cytoskeletal proteins plays a key role in cytoskeletal remodeling (Tsukita and Yonemura, 1999). Thus, we attempted to examine whether the phosphorylation state of the cytoskeletal proteins changes. When the total cell lysates prepared from Stx1-B-treated ACHN cells were examined using immunoblotting with Abs that specifically recognize Src family PTKs only when activated by phosphorylation at the C-terminal tyrosine residue, the intensification of three major bands was seen after Stx1-B treatment (Fig. 8A). Based on the molecular weights, the largest band was thought to represent the activated form of Yes, which was previously reported to appear during the course of Stx1-B-mediated activation in ACHN cells (Katagiri et al., 1999; Katagiri et al., 2001). The other smaller bands were thought to represent the activation of other Src family PTK(s) by Stx1-B stimulation. In parallel with the activation of Src family PTKs, the Stx1-B-mediated phosphorylation of both ezrin and paxillin was detected by immunoblotting with Abs that specifically recognize the phosphorylated active forms of ezrin and paxillin (Fig. 8A). The above data indicate that the Stx1-B-mediated intracellular signal induces the phosphorylation of ezrin and paxillin during the course of cytoskeletal remodeling.

As shown in Fig. 8B, the effect of Stx1-B on the induction of ezrin phosphorylation is dose-dependent and the concentration of 1 μg/ml was found to be sufficient to yield maximum effect. As shown in Fig. 8C, we also found that the treatment with anti-Gb3 Abs similarly induces the phosphorylation of ezrin in ACHN cells. Therefore, the ligation of Gb3 by pentameric Stx1-B is not always required to induce cytoskeletal signaling and the binding of monomeric forms of the ligand to Gb3 might be able to induce ezrin phosphorylation.

We also examined whether constitutive Stx1-B treatment is required to induce ezrin phosphorylation. For this purpose, we bound Stx1-B to ACHN cells on ice and then removed excess toxin by washing, before shifting the temperature to 37°C. As shown in Fig. 8D, after the temperature was shifted to 37°C, transient increase in phosphorylation of ezrin was observed by immunoblotting. Although the elevation of ezrin phosphorylation observed in this experiment is slower than that presented in Fig. 8A, it is probably due to the time lag for warming up of the medium to 37°C after the temperature shift. These data indicate that the primary ligation of the plasma membrane Gb3 pool by Stx1-B is sufficient to induce intracellular signal for cytoskeletal rearrangements.

Effect of inhibitors on Stx1-B-induced cytoskeletal remodeling

To clarify the signaling cascade that induces the phosphorylation of ezrin, we examined the effect of a number of inhibitors on Stx1-B-induced ezrin phosphorylation. As shown in Fig. 9, when ACHN cells were pre-treated with PP2, a specific inhibitor for Src family PTK, the Stx1-B-mediated phosphorylation of ezrin was clearly inhibited. Similary, MBD, which is known to disturb the structure of the lipid rafts through the depletion of cholesterol from the cell membrane,

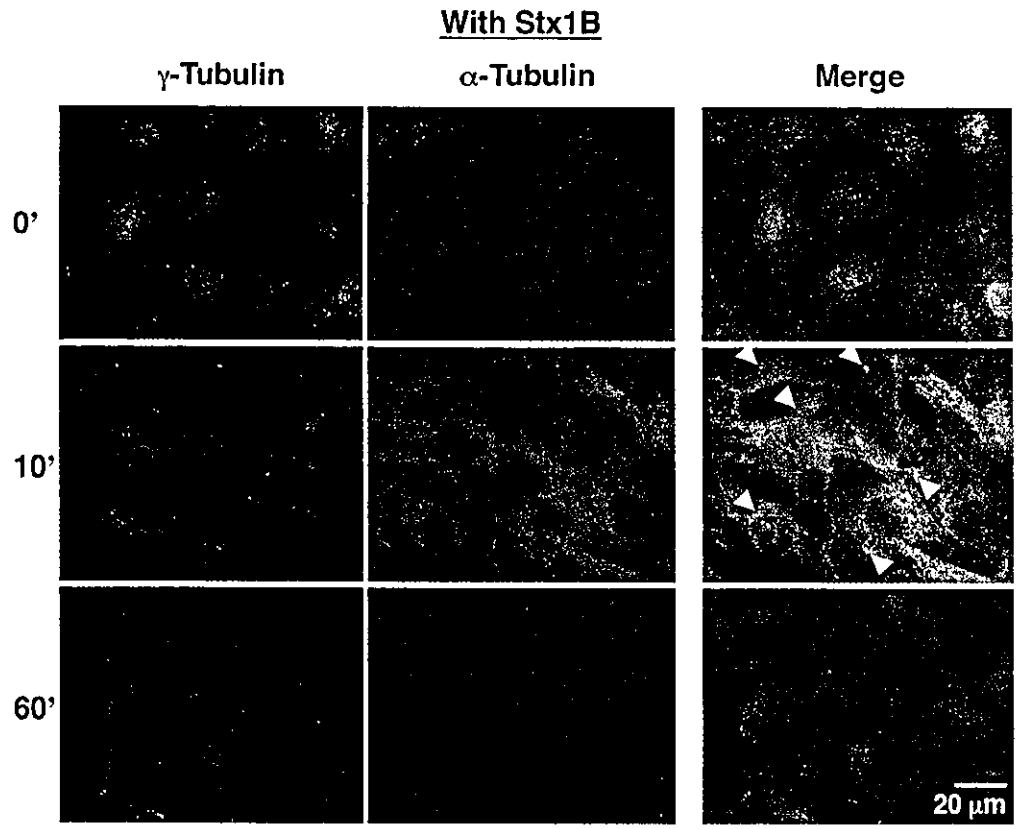

Fig. 6. Effect of Stx1-B subunit on the distribution of γ- and α-tubulins in ACHN cells. ACHN cells were examined as described in Fig. 2 using Alexa-488-labeled anti-γ-tubulin Ab (left panels, green) and Alexa-546-labeled anti-α-tubulin mAb (center panels, red). The arrowheads indicate the accumulation of γ-tubulin at the microtubule-organizing centers. Results are representative of three independent experiments.

inhibited the Stx1-B-mediated phosphorylation of ezrin (Fig. 9). In addition, LY294002, a specific inhibitor for PI3K, and Y27632, a specific inhibitor for ROCK, also inhibited the Stx1-B-mediated phosphorylation of ezrin (Fig. 9). In contrast, PKC inhibitor 20-28 (Fig. 9) and PKC inhibitor EGF-R fragment 651-658 (data not shown) did not affect the Stx1-B-mediated phosphorylation of ezrin in ACHN cells.

We next examined whether these inhibitors affect the Stx1-B-mediated cytoskeletal rearrangements. As shown in Fig. 2 and Fig. 10A, Stx1-B treatment induced the clustering of ezrin beneath the plasma membrane (indicated by arrowhead). When ACHN cells were pretreated with any of inihibitors, including PP2, MBD, LY294002 and Y27632, however, the Stx1-B-induced clustering of ezrin was not observed (Fig. 10A). Therefore, it is suggested that the inhibition of ezrin phosphorylation by these inhibitors suppresses Stx1-B-mediated redistribution of ezrin.

To clarify the molecule responsible for the redistribution of vimentin during the course of Stx1-B-induced cytoskeletal remodeling, we next examined the effect of inhibitors on the Stx1-B-induced redistribution of vimentin. As shown in Fig. 5 and Fig. 10B, Stx1-B treatment induced the accumulation of vimentin in the paranuclear area (indicated by arrowhead). When ACHN cells were pretreated with either PP2 or Y27632, however, the Stx1-B-induced clustering of vimentin in the paranuclear region was not observed (Fig. 10B), indicating the involvement of the Src family PTK and ROCK in the Stx1-B-mediated redistribution of vimentin.

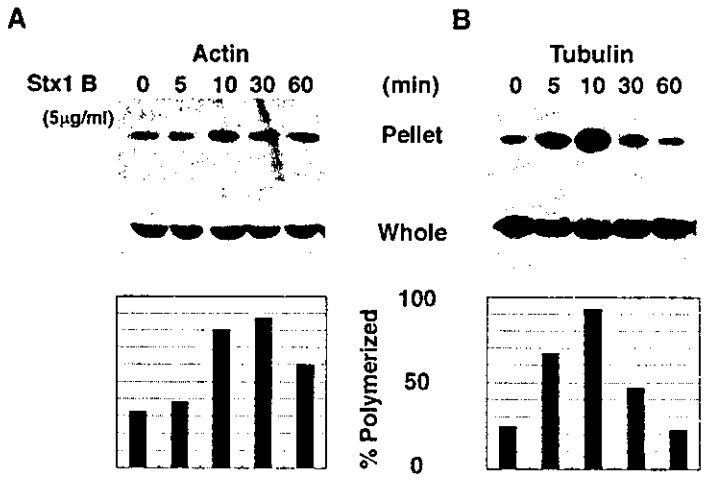

Fig. 7. Effect of Stx1-B subunit on the polymerization of actin and tubulin in ACHN cells. (A) ACHN cells were treated with and without 5 μg/ml of the Stx1-B subunit as described in Fig. 1 and lysed in the actin stabilization buffer. After removing aliquots from each whole lysate for the determination of total actin, polymerized actin (filamentous actin) was separated from soluble actin (monomer actin) by centrifugation. Both fractions of polymerized actin (pellet, upper panel) and total actin (whole, mid panel) were detected by immunoblot analysis and quantitated by densitometry. The proportion (%) polymerized was calculated by dividing the actin in the pellet fraction by the actin in the whole lysate and indicated (lower panel). (B) Tubulin polymerization was examined as in A.

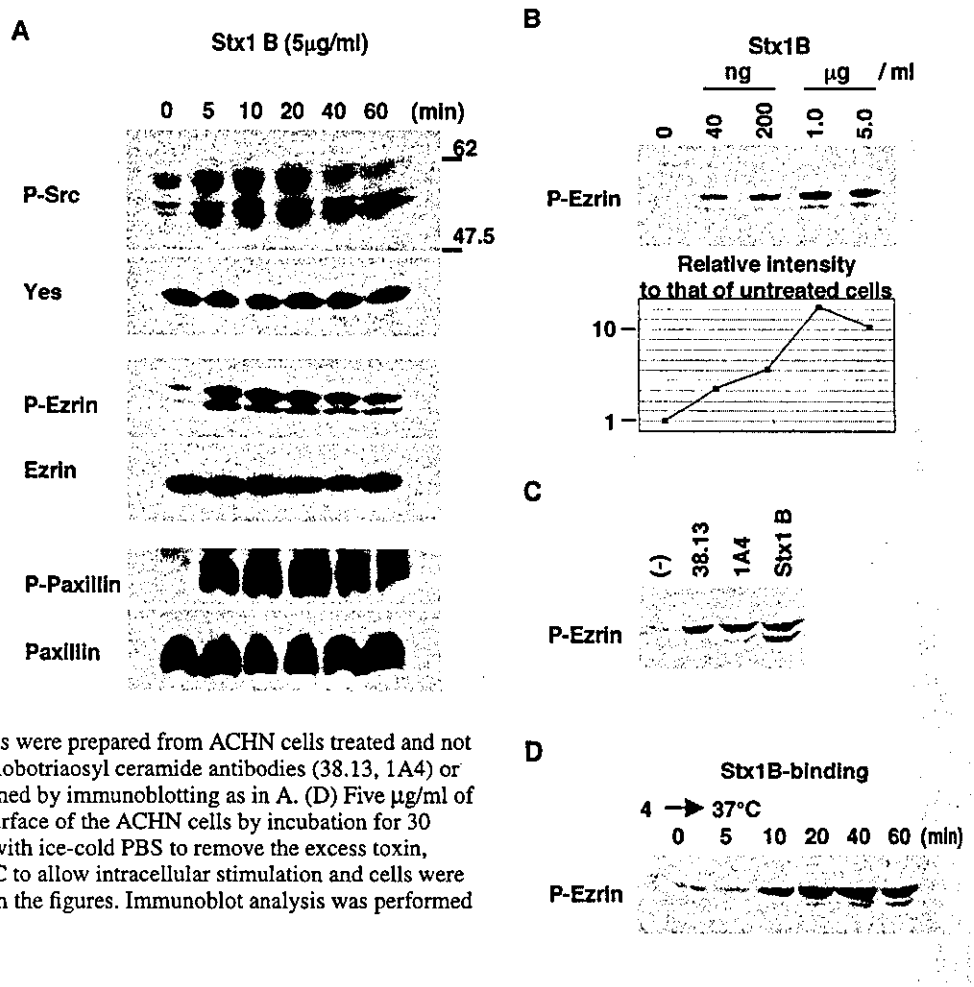

Fig. 8. Transient phosphorylation of ezrin in ACHN cells after treatment with the Stx1-B subunit. (A) Total cell extracts were prepared from ACHN cells treated with or without 5 μg/ml of Stx1-B subunit for the indicated periods. After separation on 10% SDS-PAGE gel, the proteins were transferred to a nitrocellulose membrane and immunoblotted using the indicated antibodies. (B) Total cell extracts were prepared from ACHN cells treated with or without different amounts of Stx1-B subunit for 10 minutes and immunoblot analysis was performed using anti-phospho-specific ezrin antibody (P-Ezrin) as in A. Intensity of the phospho-ezrin signals obtained from each sample was quantitated by densitometry and the relative value of each to that of untreated cells (each value/the value of untreated cells) was indicated as a graph (lower panel). (C) Total cell extracts were prepared from ACHN cells treated and not treated with 5 μg/ml each of either anti-globotriaosyl ceramide antibodies (38.13, 1A4) or Stx1-B subunit for 10 minutes and examined by immunoblotting as in A. (D) Five μg/ml of Stx1-B pentamer was bound to the cell surface of the ACHN cells by incubation for 30 minutes at 4°C. After intensive washing with ice-cold PBS to remove the excess toxin, temperature was shifted from 4°C to 37°C to allow intracellular stimulation and cells were incubated for the time periods indicated in the figures. Immunoblot analysis was performed as in A.

Discussion

In this report, we clearly demonstrated that the binding of Stx1-B induces intracellular signals that initiate cytoskeleton remodeling in ACHN renal carcinoma cells, which are related to renal tubular epithelial cells. These signals led to morphological changes and a weakened adhesiveness of the cells. The series of cellular and biological events induced by Stx1-B binding was similar to that which occurs during the course of growth factor-stimulated cell motility (Bretscher, 1989; Leventhal et al., 1997).

Several lines of evidence, including our own, have suggested that Stx directly injures renal tubular epithelial cells. For example, renal tubular epithelial cells express Gb3, which can bind Stx1 and 2 (Boyd and Lingwood, 1989; Kiyokawa et al., 1998; Taguchi et al., 1998; Uchida et al., 1999). In vitro experiments have revealed that Stx1 induces cell death in renal tubular epithelial cells through protein synthesis inhibition and apoptosis (Karpman et al., 1998; Kiyokawa et al., 1998; Taguchi et al., 1998; Williams et al., 1999). Several clinical studies have indicated the involvement of renal tubular damage during the course of HUS (Kaneko et al., 2001; Takeda et al., 1993). The appearance of apoptotic cells in the renal tubules of the kidney in HUS patients, accompanied by STEC infection, further indicates that renal tubular injury does occur in the kidneys of HUS patients (Karpman et al., 1998; Taguchi et al., 1998).

The essential cytotoxicity of Stx is generally thought to arise from the inhibition of protein synthesis by the Stx-A subunit. However, recent studies have shown that the B-subunit also has biological effects on target cells through a mechanism mediated by intracellular signals upon binding to Gb3 (Katagiri et al., 1999; Kiyokawa et al., 2001; Mangeney et al., 1993; Mori et al., 2000; Taga et al., 1997). Although Stx1-B-induced intracellular signals are known to mediate apoptosis in Burkitt's lymphoma cells, their biological effect on other cell species has not been clarified. The data presented in this study extend previous observations and indicate that Stx1-B-induced intracellular signals induce cytoskeleton remodeling, resulting in morphological changes in the target cells. As previously reported, the simultaneous addition of Stx1-B subunits enhances the cytotoxic effect of Stx1 holotoxins on ACHN cells, suggesting a synergism between A-subunit-mediated protein synthesis inhibition and B-subunit-mediated intracellular signals on the cytotoxicity observed in target cells (Katagiri et al., 2001). Although the biological significance of Stx1-B-induced cytoskeletal remodeling in target cells in vivo is not presently known, this process might participate in Stx-induced cell injury, thereby playing a role in the development of complications associated with STEC infection, such as HUS.

Gb3 acts as functional receptor for Stx, but the natural ligand of this lipid and its normal physiological role are unknown. Upon binding with its natural ligand, Gb3 might mediate intracellular signals leading to cytoskeletal remodeling,

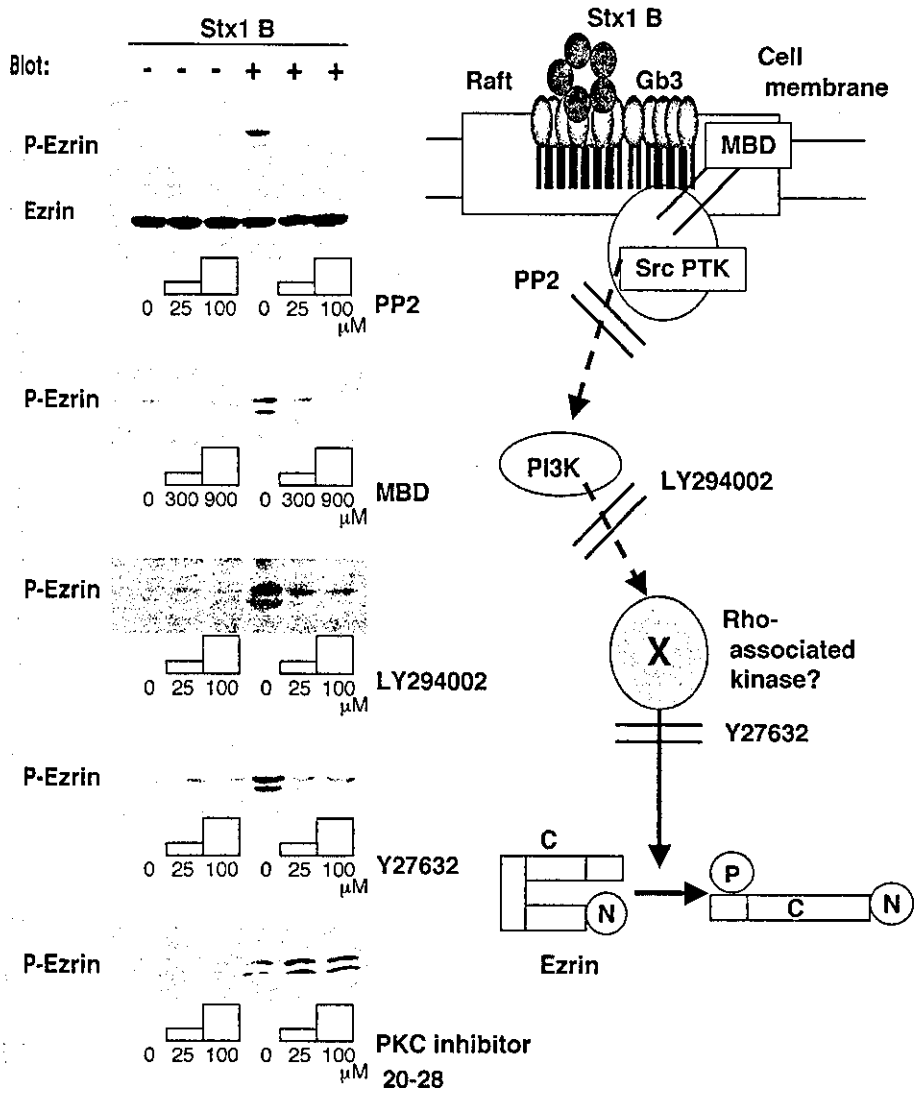

Fig. 9. Effect of inhibitors on the Stx1-B-subunit-mediated phosphorylation of ezrin. ACHN cells were preincubated with the inhibitors shown in the figure for three hours. The concentrations of 300 and 900 μM for MBD and 25 and 100 μM for other inhibitors were used. After treatment with the Stx1-B subunit for 5 minutes, cell extracts were prepared, and immunoblotting for phospho-specific ezrin was performed as described in Fig. 8. In parallel, each sample was examined using an anti-ezrin antibody to confirm that the protein amounts in each lane were comparable (only the result for PP2 is shown in the second panel from the top). In the right panel, the effect of each inhibitor is schematically presented.

participating in the development and organization of kidney tissue. Therefore, our observation might provide an in vitro model for research on lipid-receptor-mediated signaling systems for cytoskeletal remodeling.

Stx1-B binding induces the phosphorylation of ezrin, a linker protein that connects the plasma membrane and the actin cytoskeleton and is involved in cell adhesion and the formation of the free-surface domain of plasma membranes, especially in the ruffling and organization of microvilli (Berryman et al., 1995; Bretscher et al., 1997; Chen et al., 1995; Crepadi et al., 1997; Kondo et al., 1997; Takeuchi et al., 1994; Tsukita and Yonemura, 1999). Stx1-B-induced ezrin phosphorylation was inhibited both by MBD (which disturbs the structure of lipid rafts) and by the Src family PTK inihibitor PP2. Furthermore, we previously reported that Gb3 is mainly located on lipid rafts in the cell membrane, and that Stx1-B binding to Gb3 induces a clustering of the lipid rafts, leading to the activation of Src family PTK (which is anchored to the inner layer of the lipid rafts) possibly by aggregation-mediated kinase auto-phosphorylation (Katagiri et al., 1999; Mori et al., 2000). Thus, our data indicate that the lipid-raft-mediated activation of Src family PTK might play an important role in the phosphorylation of ezrin during the course of Stx-induced cytoskeleton remodeling. In addition to MBD and PP2, we also found that the inhibition of both PI3K and ROCK by their specific inhibitors abolished the Stx1-B-mediated phosphorylation of ezrin, suggesting that these molecules are located downstream from Src family PTK in the signaling cascade and participate in the Stx1-B-mediated phosphorylation of ezrin.

Several molecules have been postulated to be responsible for the phosphorylation of ezrin. For example, the Ras superfamily small G-proteins Rho, Rac and Cdc42 have been shown to be responsible for the formation of focal contact, lamellipodia and filopodia, respectively (Van Aelst and D'Souza-Schorey, 1997; Mackay and Hall, 1998). During these processes, the ERM proteins are thought to be located downstream of the small G-proteins (Bretscher et al., 1997; Matsui et al., 1998; Shaw et al., 1998; Tsukita and Yonemura, 1999). Furthermore, it has been shown that ROCK phosphorylates the C-terminal threonines of ERM proteins, regulating their head-to-tail association in in vitro experiments (Matsui et al., 1998).

We also know that myotonic dystrophy kinase-related Cdc42-binding kinase (MRCK) is a candidate for the kinase that phosphorylates ERM proteins at filopodia (Nakamura et al., 2000). In the case of Merlin, which is closely related to the ERM proteins, p21-activated kinase 2 (PAK2), a downstream effector of Rac and Cdc42, has been postulated as a candidate for the kinase that phosphorylates this protein (Kissil et al., 2002). Consistent with the above observations, we report here that the ROCK inhibitor Y27632 inhibited the Stx1-B-stimulated phosphorylation of ezrin, suggesting that ROCK is at least one of the kinases responsible for ezrin phosphorylation in Stx1-B-induced cytoskeletal remodeling. In addition, Rac and Cdc42 might also be involved in the process, as Stx1-B stimulation induces the extension of lamellipodia- and

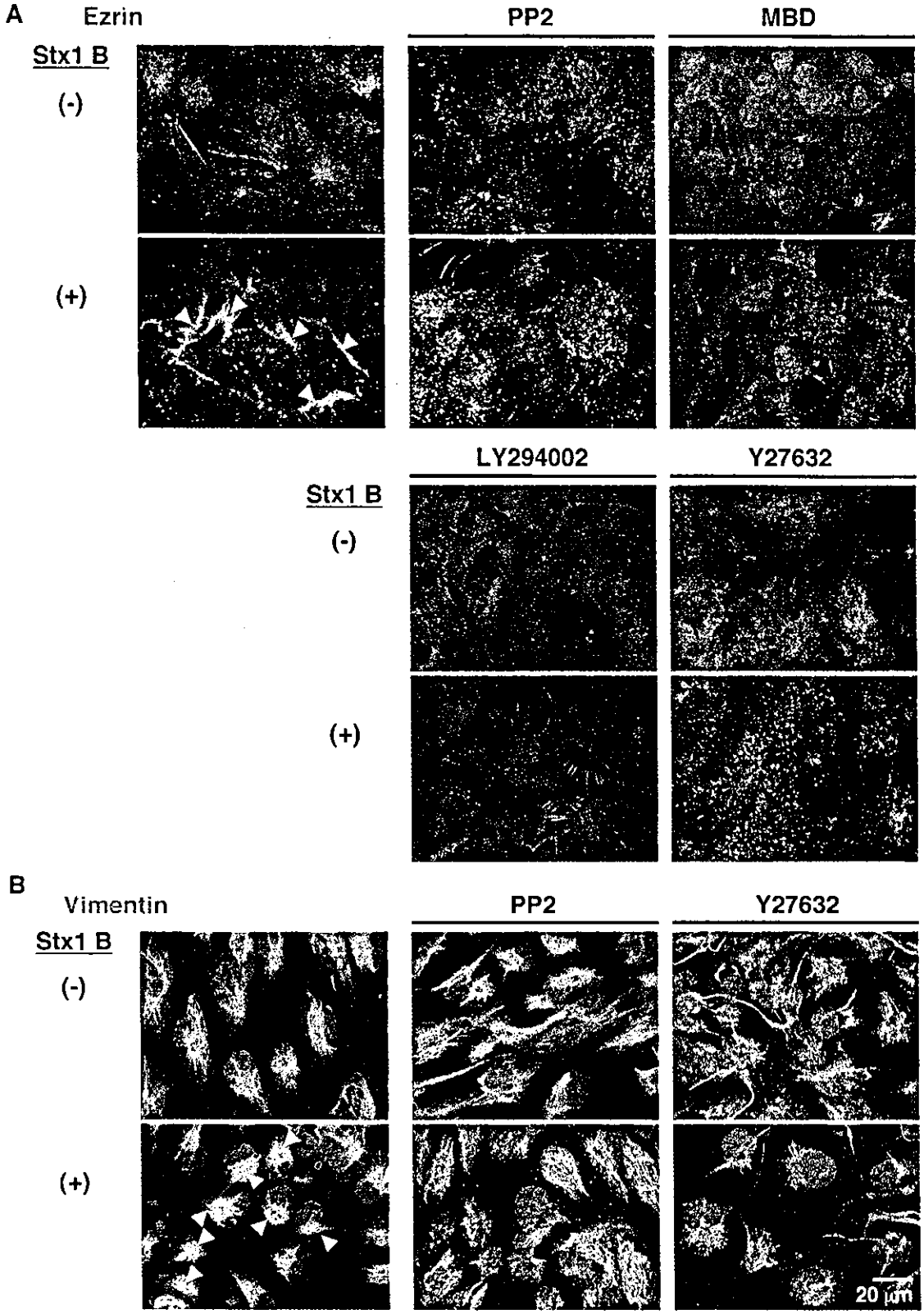

Fig. 10. Effect of inhibitors on the Stx1-B-subunit-mediated clustering of ezrin and vimentin. (A) ACHN cells were preincubated with the inhibitors shown in the figure for three hours. The concentrations of 900 μM for MBD and 100 μM for other inhibitors were used. After treatment with the Stx1-B subunit for 10 minutes, the cells were fixed and stained with anti-ezrin monoclonal antibody (green) followed by counterstaining with DAPI (blue) as in Fig. 2. Results are representative of three independent experiments. The clustering of ezrin was indicated by arrowhead. (B) ACHN cells pre-incubated with inhibitors as in A were treated with the Stx1-B for 30 minutes and stained with anti-vimentin monoclonal antibody (green) as in A.

filopodia-like structures. Further experiments investigating the involvement of small G-proteins and their downstream kinases in the Stx1-B-induced signaling system of cytoskeletal remodeling are now underway.

Conversely, it has been suggested that ezrin was a downstream effector of PKCα during the course of integrin-mediated cell migration (Ng et al., 2001). PKCθ is a major kinase specific for moesin, a family protein of ezrin (Pietromonaco et al., 1998). PKCθ is involved in regulating the localization and association of CD44 and ezrin during cell motility and invasion (Legg et al., 2002; Stapleton et al., 2002). As shown in this study, however, the PKC-inhibitors did not affect the Stx1-B-stimulated phosphorylation of ezrin. Our data might indicate that PKCs are not essential for the Stx1-B-induced phosphorylation of ezrin in our experimental system.

In addition to the phosphorylation of ezrin, we also observed changes in the distributions of several molecules, including FAK, paxillin, vimentin, cytokeratin and tubulins, all of which contribute to the organization of the cytosleleton. The molecular mechanism responsible for the above-described redistribution of cytoskeletal molecules has not yet been clarified. However, as observed in the present study, treatment with the ROCK inhibitor Y27632 abolished the Stx1-B-stimulated relocalization of vimentin, suggesting the involvement of ROCK in the Stx1-B-induced redistribution of vimentin. The ability of ROCK to phosphorylate vimentin in vitro and in vivo (Goto et al., 1998; Kosako et al., 1999) might support this idea.

In conclusion, Stx1-B-induced intracellular signals mediate the remodeling of a variety of cytoskeletal organizing proteins, resulting in changes in cell morphology. Although additional studies are clearly necessary, further investigation of the mechanism of Stx1-B-mediated cytoskeletal remodeling should provide an in vitro model for future research on the pathogenesis of Stx-mediated cell injury as well as the role of lipid raft-mediated cell signaling in cytoskeletal remodeling.

This work was supported in part by Health and Labour Sciences Research Grants from the Ministry of Health, Labour and Welfare of Japan and MEXT. KAKENHI 15019129, JSPS. KAKENHI 15390133 and 15590361. This work was also supported by a grant from the Japan Health Sciences Foundation for Research on Health Sciences Focusing on Drug Innovation. Additional support was provided by a grant from Sankyo Foundation of Life Science. We thank M. Sone and S. Yamauchi for their excellent secretarial works. We thank S. Hakomori and Otsuka Assay Laboratories for gifting anti-Gb3 mAb 1A4.

References

Andreoli, C., Martin, M., le Borgne, R., Reggio, H. and Mangeat, P. (1994). Ezrin has properties to self-associate at the plasma membrane. *J. Cell Sci.* **107**, 2509-2521.

Arpin, M., Algrain, M. and Louvard, D. (1994). Membrane-actin microfilament connections: an increasing diversity of players related to band 4.1. *Curr. Opin. Cell Biol.* **6**, 136-141.

Berryman, M., Gary, R. and Bretscher, A. (1995). Ezrin oligomers are major cytoskeletal components of placental microvilli: a proposal for their involvement in cortical morphogenesis. *J. Cell Biol.* **131**, 1231-1242.

Boyd, B. and Lingwood, C. (1989). Verotoxin receptor glycolipid in human renal tissue. *Nephron* **51**, 207-210.

Bretscher, A. (1989). Rapid phosphorylation and reorganization of ezrin and spectrin accompany morphological changes induced in A-431 cells by epidermal growth factor. *J. Cell Biol.* **108**, 921-930.

Bretscher, A., Gary, R. and Berryman, M. (1995). Soluble ezrin purified from placenta exists as stable monomers and elongated dimers with masked C-terminal ezrin-radixin-moesin association domains. *Biochemistry* **34**, 16830-16837.

Bretscher, A., Reczek, D. and Berryman, M. (1997). Ezrin: a protein requiring conformational activation to link microfilaments to the plasma membrane in the assembly of cell surface structures. *J. Cell Sci.* **110**, 3011-3018.

Burridge, K., Turner, C. E. and Romer, L. H. (1992). Tyrosine phosphorylation of paxillin and pp125FAK accompanies cell adhesion to extracellular matrix: a role in cytoskeletal assembly. *J. Cell Biol.* **119**, 893-903.

Chen, J., Cohn, J. A. and Mandel, L. J. (1995). Dephosphorylation of ezrin as an early event in renal microvillar breakdown and anoxic injury. *Proc. Natl. Acad. Sci. USA* **92**, 7495-7499.

Crepaldi, T., Gautreau, A., Comoglio, P. M., Louvard, D. and Arpin, M. (1997). Ezrin is an effector of hepatocyte growth factor-mediated migration and morphogenesis in epithelial cells. *J. Cell Biol.* **138**, 423-434.

Glogauer, M., Arora, P., Yao, G., Sokholov, I., Ferrier, J. and McCulloch, C. A. (1997). Calcium ions and tyrosine phosphorylation interact coordinately with actin to regulate cytoprotective responses to stretching. *J. Cell Sci.* **110**, 11-21.

Goto, H., Kosako, H., Tanabe, K., Yanagida, M., Sakurai, M., Amano, M., Kaibuchi, K. and Inagaki, M. (1998). Phosphorylation of vimentin by Rho-associated kinase at a unique amino-terminal site that is specifically phosphorylated during cytokinesis. *J. Biol. Chem.* **273**, 11728-11736.

Heacock, C. S. and Bamburg, J. R. (1983). The quantification of G- and F-actin in cultured cells. *Anal. Biochem.* **135**, 22-36.

Heiska, L., Alfthan, K., Gronholm, M., Vilja, P., Vaheri, A. and Carpen, O. (1998). Association of ezrin with intercellular adhesion molecule-1 and -2 (ICAM-1 and ICAM-2). Regulation by phosphatidylinositol 4, 5-bisphosphate. *J. Biol. Chem.* **273**, 21893-21900.

Hirao, M., Sato, N., Kondo, T., Yonemura, S., Monden, M., Sasaki, T., Takai, Y., Tsukita, S. and Tsukita, S. (1996). Regulation mechanism of ERM (ezrin/radixin/moesin) protein/plasma membrane association: possible involvement of phosphatidylinositol turnover and Rho-dependent signaling pathway. *J. Cell Biol.* **135**, 37-51.

Kaneko, K., Kiyokawa, N., Ohtomo, Y., Nagaoka, R., Yamashiro, Y., Taguchi, T., Mori, T., Fujimoto, J. and Takeda, T. (2001). Apoptosis of renal tubular cells in Shiga-toxin-mediated hemolytic uremic syndrome. *Nephron* **87**, 182-185.

Kaplan, B. S., Cleary, T. G. and Obrig, T. G. (1990). Recent advances in understanding the pathogenesis of the hemolytic uremic syndromes. *Pediatr. Nephrol.* **4**, 276-283.

Karpman, D., Hakansson, A., Perez, M. T., Isaksson, C., Carlemalm, E., Caprioli, A. and Svanborg, C. (1998). Apoptosis of renal cortical cells in the hemolytic-uremic syndrome: in vivo and in vitro studies. *Infect. Immun.* **66**, 636-644.

Katagiri, U. Y., Mori, T., Nakajima, H., Katagiri, C., Taguchi, T., Takeda, T., Kiyokawa, N. and Fujimoto, J. (1999). Activation of Src family kinase Yes induced by Shiga toxin binding to globotriaosyl ceramide (Gb3/CD77) in low density, detergent-insoluble microdomains. *J. Biol. Chem.* **274**, 35278-35282.

Katagiri, U. Y., Kiyokawa, N. and Fujimoto, J. (2001). The effect of Shiga toxin binding to globotriaosylceramide in rafts of human kidney cells and Burkitt's lymphomaa cells. *Trends. Glycosci. Glycotech.* **13**, 281-290.

Kissil, J. L., Johnson, K. C., Eckman, M. S. and Jacks, T. (2002). Merlin phosphorylation by p21-activated kinase 2 and effects of phosphorylation on merlin localization. *J. Biol. Chem.* **277**, 10394-10399.

Kiyokawa, N., Taguchi, T., Mori, T., Uchida, H., Sato, N., Takeda, T. and Fujimoto, J. (1998). Induction of apoptosis in normal human renal tubular epithelial cells by *Escherichia coli* Shiga toxins 1 and 2. *J. Infect. Dis.* **178**, 178-184.

Kiyokawa, N., Mori, T., Taguchi, T., Saito, M., Mimori, K., Suzuki, T., Sekino, T., Sato, N., Nakajima, H., Katagiri, Y. U. et al. (2001). Activation of the caspase cascade during Stx1-induced apoptosis in Burkitt's lymphoma cells. *J. Cell. Biochem.* **81**, 128-142.

Knowles, G. C. and McCulloch, C. A. (1992). Simultaneous localization and quantification of relative G and F actin content: optimization of fluorescence labeling methods. *J. Histochem. Cytochem.* **40**, 1605-1612.

Kojio, S., Zhang, H., Ohmura, M., Gondaira, F., Kobayashi, N. and Yamamoto, T. (2000). Caspase-3 activation and apoptosis induction coupled with the retrograde transport of shiga toxin: inhibition by brefeldin A. *FEMS Immunol. Med. Microbiol.* **29**, 275-281.

Kondo, T., Takeuchi, K., Doi, Y., Yonemura, S., Nagata, S. and Tsukita, S. (1997). ERM (ezrin/radixin/moesin)-based molecular mechanism of microvillar breakdown at an early stage of apoptosis. *J. Cell Biol.* **139**, 749-758.

Kosako, H., Goto, H., Yanagida, M., Matsuzawa, K., Fujita, M., Tomono, Y., Okigaki, T., Odai, H., Kaibuchi, K. and Inagaki, M. (1999). Specific accumulation of Rho-associated kinase at the cleavage furrow during cytokinesis: cleavage furrow-specific phosphorylation of intermediate filaments. *Oncogene* **18**, 2783-2788.

Legg, J. W., Lewis, C. A., Parsons, M., Ng, T. and Isacke, C. M. (2002). A novel PKC-regulated mechanism controls CD44 ezrin association and directional cell motility. *Nat. Cell Biol.* **4**, 399-407.

Leventhal, P. S., Shelden, E. A., Kim, B. and Feldman, E. L. (1997). Tyrosine phosphorylation of paxillin and focal adhesion kinase during insulin-like growth factor-I-stimulated lamellipodial advance. *J. Biol. Chem.* **272**, 5214-5218.

Lingwood, C. A. (1996). Role of verotoxin receptors in pathogenesis. *Trends Microbiol.* **4**, 147-153.

Mackay, D. J. and Hall, A. (1998). Rho GTPases. *J. Biol. Chem.* **273**, 20685-20688.

Mangeney, M., Lingwood, C. A., Taga, S., Caillou, B., Tursz, T. and Wiels, J. (1993). Apoptosis induced in Burkitt's lymphoma cells via Gb3/CD77, a glycolipid antigen. *Cancer Res.* **53**, 5314-5319.

Matsui, T., Maeda, M., Doi, Y., Yonemura, S., Amano, M., Kaibuchi, K., Tsukita, S. and Tsukita, S. (1998). Rho-kinase phosphorylates COOH-terminal threonines of ezrin/radixin/moesin (ERM) proteins and regulates their head-to-tail association. *J. Cell Biol.* **140**, 647-657.

McCormack, S. A., Ray, R. M., Blanner, P. M. and Johnson, L. R. (1999). Polyamine depletion alters the relationship of F-actin, G-actin, and thymosin beta4 in migrating IEC-6 cells. *Am. J. Physiol.* **276**, C459-C468.

Minotti, A. M., Barlow, S. B. and Cabral, F. (1991). Resistance to antimitotic drugs in Chinese hamster ovary cells correlates with changes in the level of polymerized tubulin. *J. Biol. Chem.* **266**, 3987-3994.

Montgomery, R. B., Guzman, J., O'Rourke, D. M. and Stahl, W. L. (2000). Expression of oncogenic epidermal growth factor receptor family kinases induces paclitaxel resistance and alters beta-tubulin isotype expression. *J. Biol. Chem.* **275**, 17358-17363.

Mori, T., Kiyokawa, N., Katagiri, Y. U., Taguchi, T., Suzuki, T., Sekino, T., Sato, N., Ohmi, K., Nakajima, H., Takeda, T. et al. (2000). Globotriaosyl ceramide (CD77/Gb3) in the glycolipid-enriched membrane domain participates in B-cell receptor-mediated apoptosis by regulating lyn kinase activity in human B cells. *Exp. Hematol.* **28**, 1260-1268.

Moritz, M. and Agard, D. A. (2001). γ-tubulin complexes and microtubule nucleation. *Curr. Opin. Struct. Biol.* **11**, 174-181.

Nakajima, H., Katagiri, Y. U., Kiyokawa, N., Taguchi, T., Suzuki, T., Sekino, T., Mimori, K., Saito, M., Nakao, H., Takeda, T. et al. (2001). Single-step method for purification of Shiga toxin-1 B subunit using receptor-mediated affinity chromatography by globotriaosylceramide-conjugated octyl sepharose CL-4B. *Protein Expr. Purif.* **22**, 267-275.

Nakamura, N., Oshiro, N., Fukata, Y., Amano, M., Fukata, M., Kuroda, S., Matsuura, Y., Leung, T., Lim, L. and Kaibuchi, K. (2000). Phosphorylation of ERM proteins at filopodia induced by Cdc42. *Gene. Cell.* **5**, 571-581.

Ng, T., Parsons, M., Hughes, W. E., Monypenny, J., Zicha, D., Gautreau, A., Arpin, M., Gschmeissner, S., Verveer, P. J., Bastiaens, P. I. et al. (2001). Ezrin is a downstream effector of trafficking PKC-integrin complexes involved in the control of cell motility. *EMBO J.* **20**, 2723-2741.

Pietromonaco, S. F., Simons, P. C., Altman, A. and Elias, L. (1998). Protein kinase C-theta phosphorylation of moesin in the actin-binding sequence. *J. Biol. Chem.* **273**, 7594-7603.

Richardson, S. E., Karmali, M. A., Becker, L. E. and Smith, C. R. (1988). The histopathology of the hemolytic uremic syndrome associated with verocytotoxin-producing *Escherichia coli* infections. *Hum. Pathol.* **19**, 1102-1108.

Rodgers, W. and Rose, J. K. (1996). Exclusion of CD45 inhibits activity of p56lck associated with glycolipid-enriched membrane domains. *J. Cell Biol.* **135**, 1515-1523.

Serrador, J. M., Alonso-Lebrero, J. L., del Pozo, M. A., Furthmayr, H., Schwartz-Albiez, R., Calvo, J., Lozano, F. and Sanchez-Madrid, F. (1997). Moesin interacts with the cytoplasmic region of intercellular adhesion molecule-3 and is redistributed to the uropod of T lymphocytes during cell polarization. *J. Cell Biol.* **138**, 1409-1423.

Shaw, R. J., Henry, M., Solomon, F. and Jacks, T. (1998). RhoA-dependent phosphorylation and relocalization of ERM proteins into apical membrane/actin protrusions in fibroblasts. *Mol. Biol. Cell* **9**, 403-419.

Simons, K. and Ikonen, E. (1997). Functional rafts in cell membranes. *Nature* **387**, 569-572.

Stapleton, G., Malliri, A. and Ozanne, B. W. (2002). Downregulated AP-1 activity is associated with inhibition of protein-kinase-C-dependent CD44 and ezrin localisation and upregulation of PKC theta in A431 cells. *J. Cell Sci.* **115**, 2713-2724.

Taga, S., Carlier, K., Mishal, Z., Capoulade, C., Mangeney, M., Lecluse, Y., Coulaud, D., Tetaud, C., Pritchard, L. L., Tursz, T. et al. (1997). Intracellular signaling events in CD77-mediated apoptosis of Burkitt's lymphoma cells. *Blood* **90**, 2757-2767.

Taguchi, T., Uchida, H., Kiyokawa, N., Mori, T., Sato, N., Horie, H., Takeda, T. and Fujimoto, J. (1998). Verotoxins induce apoptosis in human renal tubular epithelium derived cells. *Kidney Int.* **53**, 1681-1688.

Takeda, T., Dohi, S., Igarashi, T., Yamanaka, T., Yoshiya, K. and Kobayashi, N. (1993). Impairment by verotoxin of tubular function contributes to the renal damage seen in haemolytic uraemic syndrome. *J. Infect.* **27**, 339-341.

Takeuchi, K., Sato, N., Kasahara, H., Funayama, N., Nagafuchi, A., Yonemura, S., Tsukita, S. and Tsukita, S. (1994). Perturbation of cell adhesion and microvilli formation by antisense oligonucleotides to ERM family members. *J. Cell Biol.* **125**, 1371-1384.

Tsukita, S. and Yonemura, S. (1997). ERM (ezrin/radixin/moesin) family: from cytoskeleton to signal transduction. *Curr. Opin. Cell Biol.* **9**, 70-75.

Tsukita, S. and Yonemura, S. (1999). Cortical actin organization: lessons from ERM (ezrin/radixin/moesin) proteins. *J. Biol. Chem.* **274**, 34507-34510.

Tsukita, S., Oishi, K., Sato, N., Sagara, J., Kawai, A. and Tsukita, S. (1994). ERM family members as molecular linkers between the cell surface glycoprotein CD44 and actin-based cytoskeletons. *J. Cell Biol.* **126**, 391-401.

Tsukita, S., Yonemura, S. and Tsukita, S. (1997). ERM proteins: head-to-tail regulation of actin-plasma membrane interaction. *Trends. Biochem. Sci.* **22**, 53-58.

Turunen, O., Wahlstrom, T. and Vaheri, A. (1994). Ezrin has a COOH-terminal actin-binding site that is conserved in the ezrin protein family. *J. Cell Biol.* **126**, 1445-1453.

Uchida, H., Kiyokawa, N., Horie, H., Fujimoto, J. and Takeda, T. (1999). The detection of Shiga toxins in the kidney of a patient with hemolytic uremic syndrome. *Pediatr. Res.* **45**, 133-137.

Van Aelst, L. and D'Souza-Schorey, C. (1997). Rho GTPases and signaling networks. *Genes. Dev.* **11**, 2295-2322.

Williams, J. M., Lea, N., Lord, J. M., Roberts, L. M., Milford, D. V. and Taylor, C. M. (1997). Comparison of ribosome-inactivating proteins in the induction of apoptosis. *Toxicol. Lett.* **91**, 121-127.

Williams, J. M., Boyd, B., Nutikka, A., Lingwood, C. A., Barnett-Foster, D. E., Milford, D. V. and Taylor, C. M. (1999). A comparison of the effects of verocytotoxin-1 on primary human renal cell cultures. *Toxicol. Lett.* **105**, 47-57.

Yonemura, S., Nagafuchi, A., Sato, N. and Tsukita, S. (1993). Concentration of an integral membrane protein, CD43 (leukosialin, sialophorin), in the cleavage furrow through the interaction of its cytoplasmic domain with actin-based cytoskeletons. *J. Cell Biol.* **120**, 437-449.

Immunology 2004 **112** 575–582 doi:10.1111/j.1365-2567.2004.01918.x

Deficiency of BLNK hampers PLC-γ2 phosphorylation and Ca^{2+} influx induced by the pre-B-cell receptor in human pre-B cells

TOMOKO TAGUCHI,*† NOBUTAKA KIYOKAWA,* HISAMI TAKENOUCH,* JUN MATSUI,* WEI-RAN TANG,* HIDEKI NAKAJIMA,* KYOKO SUZUKI,* YUSUKE SHIOZAWA,* MASAHIRO SAITO,* YOHKO U. KATAGIRI,* TAKAO TAKAHASHI,† HAJIME KARASUYAMA,‡ YOSHINOBU MATSUO,§ HAJIME OKITA,* & JUNICHIRO FUJIMOTO* *Department of Developmental Biology, National Research Institute for Child Health and Development, Setagaya-ku, Tokyo, †Department of Pediatrics, Keio University, School of Medicine, Shinjuku-ku, Tokyo, ‡Department of Immune Regulation, Tokyo Medical and Dental University, Graduate School, Tokyo, and §Fujisaki Cell Center, Hayashibara Biochemical Laboratories Inc, Fujisaki, Okayama, Japan

SUMMARY

B-cell linker protein (BLNK) is a component of the B-cell receptor (BCR) as well as of the pre-BCR signalling pathway, and $BLNK^{-/-}$ mice have a block in B lymphopoiesis at the pro-B/pre-B cell stage. A recent report described the complete loss or drastic reduction of BLNK expression in approximately 50% of human childhood pre-B acute lymphoblastic leukaemias (ALL), therefore we investigated BLNK expression in human pre-B ALL cell lines. One of the four cell lines tested, HPB-NULL cells, was found to lack BLNK expression, and we used these human pre-B ALL cell lines that express and do not express BLNK to investigate the intracellular signalling events following pre-BCR cross-linking. When pre-BCR was cross-linked with anti-μ heavy-chain antibodies, significant phosphorylation of intracellular molecules, including Syk, Shc, ERK MAP kinase, and AKT, and an activation of Ras were observed without regard to deficiency of BLNK expression, suggesting that BLNK is not required for pre-BCR-mediated activation of MAP kinase and phosphatidyl-inositol 3 (PI3) kinase signalling. By contrast, phospholipase C-γ2 (PLC-γ2) phosphorylation and an increase in intracellular Ca^{2+} level mediated by pre-BCR cross-linking were observed only in the BLNK-expressing cells, indicating that BLNK is essential for PLC-γ2-induced Ca^{2+} influx. Human pre-B cell lines expressing and not expressing BLNK should provide an *in vitro* model for investigation of the role of BLNK in the pre-BCR-mediated signalling mechanism.

Keywords B-cell receptor; B cells; signalling/signal transduction

INTRODUCTION

Signals transduced through antigen receptors play essential roles in B-cell development and fate determination. The B-cell antigen receptor (BCR), which consists of a μ heavy chain (HC), conventional light chain (LC), immunoglobulin α (Igα; CD79a), and Igβ (CD79b), mediates different biological responses in B cells, i.e. proliferation, differentiation, growth arrest, or induction of apoptosis, depending on the differentiation and activation stage of the B cell.[1–3]

In contrast to mature B cells, B-cell progenitors do not possess the complete forms of the BCR, but do express BCR-related components. For example, pro-B cells express the Igα/Igβ heterodimer in association with calnexin,[4] an integral membrane protein, and the surrogate light (SL) chain encoded by the VpreB (CD179a) and λ5 (CD179b) genes.[5,6] These molecules have been found to be competent for transducing differentiation signals for pro-B cells.[4]

In addition, pre-B cells that have successfully accomplished rearrangement of the HC genes start to express a premature form of the antigen receptor, i.e. a pre-B-cell

Received 15 December 2004; revised 21 April 2004; accepted 10 May 2004.

Correspondence: Dr Nobutaka Kiyokawa, Department of Developmental Biology, National Research Institute for Child Health and Development, 3-35-31, Taishido, Setagaya-ku, Tokyo 154–8567, Japan. E-mail: nkiyokawa@nch.go.jp

receptor (pre-BCR) consisting of μ HC, SL chains and the Igα/Igβ heterodimers.[7–9] Several studies have shown the vital importance of pre-BCR as a mediator of pre-B-cell differentiation signals.[10–12] Expression of pre-BCR on the cell surface suppresses further recombination of μ HC genes and induces rearrangement of the conventional LC genes, indicating that signals through pre-BCR facilitate the proliferation of successfully developed pre-B cells.

Although the μ HC does not have any enzymatic activity in its cytoplasmic domain to transduce intracellular signals, the regulatory cascade of molecules is involved in BCR-mediated signalling.[2,3] The stimuli conveyed by antigens through BCR activate a number of BCR-associated cytoplasmic protein tyrosine kinases (PTKs), including the Src-family PTKs, Syk and Brutons tyrosine kinase (BTK).[13,14] These PTKs then phosphorylate numerous intracellular proteins and couple BCR stimulation to intracellular signallings, such as phosphoinositide hydrolysis, protein kinase C activation, and activation of Ras-mitogen-activated protein (MAP) kinase pathways.[2,3] A similar molecular cascade for signal transduction has been postulated for pre-BCR signalling.[4,15]

B-cell linker protein (BLNK), also known as SLP-65, BASH and BCA, is a B-cell adaptor molecule that links the cytoplasmic PTKs with phosphorylation of downstream effector molecules[16–18] and plays a crucial role in the BCR signalling system. Since BLNK does not encode any intrinsic enzymatic activity, its function is to serve as a scaffold for assembling molecular complexes that include enzymes and additional linker proteins. Upon BCR stimulation, BLNK couples activated Syk to phospholipase C-γ (PLC-γ), Vav, Grb2 and NCK.[19] In addition, it binds Btk[20,21] and is required for activation of the transcription factor NF-κB.[22] It has been reported consistently that B cells lacking BLNK fail to elicit Ca^{2+} influx following BCR cross-linking and exhibit attenuated activation of all three families of MAP kinases.[19]

BLNK has also been shown to play important roles in pre-BCR signalling, and BLNK-deficient mice show a partial block at the pre-B cell stage characterized by impaired developmental progression from large cycling $CD43^+$ pro-B cells into small resting $CD43^-$ pre-B cells,[23–26] suggesting an essential role of BLNK in pre-BCR signalling that mediates the growth and differentiation of B-cell precursors.

More importantly, it has been reported that some BLNK-deficient mice spontaneously develop pre-B-cell lymphomas that express large amounts of pre-BCR on their surface.[27,28] Consistent with this, approximately 50% of human childhood pre-B acute lymphoblastic leukaemias (ALL) show complete loss or drastic reduction of BLNK expression.[29] These findings indicate that BLNK functions as a tumour suppressor and that loss of BLNK and the accompanying block in pre-B-cell differentiation is one of the primary causes of pre-B ALL, although the precise mechanism is unknown.

We employed human pre-B cell lines that express and do not express BLNK and examined the intracellular signalling events following pre-BCR cross-linking in an attempt to investigate the role of BLNK in pre-BCR-mediated signalling. In this paper, we report the absence of Ca^{2+} influx following pre-BCR ligation in BLNK-negative human pre-B-cell lines, but not interference with pre-BCR-mediated phosphorylation of intracellular molecules. This suggests that BLNK is essential to Ca^{2+} signalling in human pre-B cells but not to other signalling cascades and it should provide an *in vitro* model for studying the role of BLNK in pre-BCR-mediated signalling.

MATERIALS AND METHODS

Cells and reagents

The human pre-B cell lines, NALM-17, HPB-NULL, P30/OHK[30] and NALM-6[31] were used in this study. The cells were cultured in RPMI-1640 supplemented with 10% fetal calf serum at 37° in a humidified 5% CO_2 atmosphere. The mouse monoclonal antibodies (mAbs) used were; anti-μ (G20-127), anti-κ (G20-193), and anti-λ (JDC-12) from Pharmingen (San Diego, CA); anti-BLNK (2B11), anti-Syk (4D10), and anti PLC-γ2 (B-10), from Santa Cruz Biotechnology (Santa Cruz, CA); anti-extracellular signal-regulated kinase (ERK)-1 (MK12) from Transduction Laboratories (Lexington, KY); anti-phosphotyrosine (PY) (4G10) from Upstate Biotechnology Inc. (Lake Placid, NY); anti-μ (AF6) from Beckman/Coulter Inc. (Westbrook, MA); anti-β actin (ZSA1) from Seikagaku Co. (Tokyo, Japan); and anti-μ (DA4.4) from the American Type Culture Collection (Rockville, MD). Anti-λ5 (HSL11), anti-Vpre-B (HSL96) and anti-conformational pre-BCR (HSL2) were also used.[30] As the negative control for flow cytometric analysis, isotype-matched mouse immunoglobulins, IgG1 (KOPC-31C) and IgG2a (G155-178), from Pharmingen were used. The rabbit polyclonal antibodies used were; $F(ab')_2$ fragment of anti-μ HC from Jackson Laboratory, Inc. (West Grove, PA); anti-PLC-γ1, anti-phospho-ERK, anti-phospho-MAP kinase/ERK kinase (MEK), anti-phospho-PLC-γ1, anti-phospho-PLC-γ2 and anti-phospho-AKT from New England Biolabs, Inc. (Beverly, MA); anti-PLC-γ2 from Pharmingen; and anti-Shc from Transduction Laboratories. The goat polyclonal anti-BTK antibody from Santa Cruz Biotechnology was also used. Secondary antibodies, including fluorescein-conjugated and enzyme-conjugated antibodies, were purchased from Jackson.

Immunofluorescence study

The cells were stained with mAbs and analysed by flow cytometry (EPICS-XL, Coulter) as described previously.[32] Staining of cytoplasmic antigens was performed with CytoStain™ Kits (Pharmingen) according to the manufacturer's protocol.

Immunoblotting and immunoprecipitation

Immunoblotting was performed as described previously.[33] Briefly, cell lysates were prepared by solubilizing the cells in lysis buffer (containing 20 mM Na_2PO_4, pH 7·4, 150 mM NaCl, 1% Triton X-100, 1% aprotinin, 5 mM phenylmethylsulphonyl fluoride, 100 mM NaF and 2 mM Na_3VO_4). After centrifugation, supernatants were obtained and the protein concentration of each cell lysate was